NON-TECHNICAL LOSS FRAUD DETECTION IN SMART GRID

by

WENLIN HAN

YANG XIAO, COMMITTEE CHAIR
XIAOYAN HONG
SUSAN VRBSKY
JINGYUAN ZHANG
O'NEILL ZHENG

A DISSERTATION

Submitted in partial fulfillment of the requirements
for the degree of Doctor of Philosophy
in the Department of Computer Science
in the Graduate School of
The University of Alabama

TUSCALOOSA, ALABAMA

2017

ABSTRACT

Utility companies consistently suffer from the harassing of Non-Technical Loss (NTL) frauds globally. In the traditional power grid, electricity theft is the main form of NTL frauds. In Smart Grid, smart meter thwarts electricity theft in some ways but cause more problems, e.g., intrusions, hacking, and malicious manipulation. Various detectors have been proposed to detect NTL hhfrauds including physical methods, intrusion-detection based methods, profile-based methods, statistic methods and comparison-based methods. However, these methods either rely on user behavior analysis which requires a large amount of detailed energy consumption data causing privacy concerns or need a lot of extra devices which are expensive. Or they have some other problems. In this dissertation, we thoroughly study NTL frauds in Smart Grid. We thoroughly survey the existing solutions and divided them into five categories. After studying the problems of the existing solutions, We propose three novel detectors to detect NTL frauds in Smart Grid which can address the problems of all the existing solutions. These detectors model an adversary's behavior and detect NTL frauds based on several numerical analysis methods which are lightweight and non-traditional. The first detector is named NTL Fraud Detection (NFD) which is based on Lagrange polynomial. NFD can detect a single tampered meter as well as multiple tampered meters in a group. The second detector is based on Recursive Least Square (RLS), which is named Fast NTL Fraud Detection (FNFD). FNFD is proposed to improve the detection speed of NFD. Colluded NTL Fraud Detection (CNFD) is the third detector that we propose to detect colluded NTL frauds. We have also studied the parameter selection and performance of these detectors.

DEDICATION

I dedicate my Ph.D dissertation to my supervisor, Dr. Yang Xiao, and other dissertation committee members, Dr. Xiaoyan Hong, Dr. Susan Vrbsky, Dr. Jingyuan Zhang and Dr. O'neill Zheng. Their support was to different extents and along with many other persons crucial for the completion of my dissertation.

I would like to express my deepest gratitude to the dean, Dr. David Cordes, and other faculty and staff in Computer Science department who offered collegial guidance and support over the years.

I would like to extend my thanks to my family and the many friends who supported me on this journey.

LIST OF ABBREVIATIONS AND SYMBOLS

A	The array of all coefficients
A_j	The estimation of A after j times of measurements
$\alpha_{i,j}$	The accuracy ratio of Meter i during T_j
α_{max}	The upper limit of the accuracy ratio of Meter i during T_j
α_{min}	The lower limit of the accuracy ratio of Meter i during T_j
AMI	Advanced Metering Infrastructure
CNFD	Colluded NTL Fraud Detection
e	The user defined error
$E_{i,j}$	The unit of electricity consumed by a consumer i during T_j
E_j	The total unit of electricity recorded by the observer meter in T_j
E_T	The matrix of E_j
FNFD	Fast NTL Fraud Detection
I	The identity matrix
i	The numbering of meters
IDS	Intrusion Detection Systems
j	The numbering of time intervals
k	A constant with a high value
λ	A forgetting factor which has a value between 0 and 1
m	The order of the Lagrange polynomial
m_{max}	The maximum order of the Lagrange polynomial
N	The total number of meters in a community

n	The number of meters in one observation group
NCG	Non-cooperative Game
NFD	NTL Fraud Detection
NTL	Non-Technical Loss
o	The number of the observer meters installed in a community
OPF	Optimum-Path Forest
P	The degree of precision of the measurement
PLC	Power Line Carrier
$r_{i,j}$	The distance from a point to the closest line of Meter i in T_j
RLS	Recursive Least Square
S	The summation of the distances r_{ij}
SCADA	Supervisory Control and Data Acquisition System
T_j	The measured time intervals
W	The array of weight
w_1	The weight of the detection time
w_2	The weight of the number of the observer meters
X	The matrix of $x_{i,j}$
$x_{i,j}$	The unit of billed electricity, which is recorded by Meter i during T_j

ACKNOWLEDGMENTS

This work was partially supported by the National Science Foundation (NSF) under grant CNS-1059265.

CONTENTS

LIST OF TABLES

LIST OF FIGURES

CHAPTER 1

INTRODUCTION

Smart Grid has the capability of two-way communication and two-way electricity flow, and this could be utilized by an adversary to manipulate any smart meter. When a smart meter is manipulated by an adversary to gain illegal benefit and cause economic loss to the utility, a Non-Technical Loss (NTL) fraud occurs. The economic loss has been caused by NTL frauds is huge. In developed countries, such as United State, the annual loss is $6 billion [44]. In developing countries, the annual loss due to NTL frauds is $58.7 billion, which is reported in a study of the top 50 emerging market countries, published by northeast group, llc in 2014 [6]. These countries, including China, India, etc., will invest $168 billion to deal with NTL frauds and build reliable Smart Grid till 2034.

NTL frauds have existed for a long time in the power grids, not only in Smart Grid. The main form of NTL frauds is "stealing electricity" in the traditional power grid [41]. The main methods are physical methods such as slowing down an analog meter by adding sand into it. In Smart Grid, smart meters are digital meters with built-in programs to process and store data. In the communication networks of Smart Grid, every device can communicate with another device in the networks, and these devices include smart meters, home appliances, substations, head-end devices, etc. The malicious behavior of adversaries are extended from a single meter to all the devices and channels in the networks. Besides interrupting measurement, adversaries have two more ways to commit NTL frauds: tampering with meters and intruding networks. They can remotely manipulate a smart meter or even multiple smart meters simultaneously. Or they can intercept the communication networks and inject falsified data into messages. NTL frauds are not attacks, but they have a close relationship with attacks, including message manipulation,

key spoofing, impersonation attack, etc., in Smart Grid. In the traditional power grid, an NTL fraud may last for a few months or longer, since the physical method that it relies on is not easily withdrawn. For example, it is easy to add sand into a meter, but not easy to take it out. This feature gives plenty of time to the utility to investigate an NTL fraud case. Nevertheless, NTL frauds are much faster, more flexible and more complicated in Smart Grid, therefore this challenges the detection speed of the existing schemes.

Various schemes have been proposed to detect NTL frauds, and they can be divided into physical methods, intrusion-detection based methods, profile-based methods, statistic methods and comparison-based methods. Existing physical methods include video survalliance, power line inspection, etc. [10, 47] and they are expensive and inefficient. Typical methods based on user profile analysis include machine learning, data mining, etc. [12, 14, 43]. They have to analyze large volumes of detailed energy consumption data. Typical IDS [18, 45] in Smart Grid are not introduced to detect NTL frauds but to deal with security issues in Smart Grid generally. In the existing comparison-based methods [58, 59, 61], they can detect NTL frauds with a small amount of data, but the detection speed still needs improvement. Statistic methods [35, 40] suffer from high false alarm rate caused by variations such as change of weather, new home appliances, etc.

In this dissertation, we will introduce three novel detectors that we proposed to detect NTL frauds in Smart Grid, which are NFD [26, 31], FNFD [28, 29] and CNFD [21, 32]. NFD can detect NTL frauds with only a small amount of data and one additional device. NFD is based on Lagrange polynomial to model an adversary's behaviors, and detect a tampered meter by comparing the difference between the results. Different from the existing detectors, our detector knows adversaries better than adversaries themselves. By building mathematical models of these adversaries, we can predict their behaviors which they may not be aware of by themselves. NFD makes it practical to detect NTL frauds both online and offline in Smart Grid. NFD can facilitate real-world applications before Smart Grid is fully deployed since it can serve the traditional

power grid and Smart Grid simultaneously. Experimental results show the effectiveness of NFD. It can detect multiple tampered meters and multiple adversaries, as well as a single tampered meter and a single adversary. We also study how to tune the parameters used in NFD to further guide its practical usage.

FNFD is a fast NTL fraud detector which is proposed to improve the detection speed of NFD and the other existing detectors. FNFD is based on Recursive Least Square (RLS) to model adversary behavior. Experimental results show that FNFD outperforms the existing schemes regarding detection speed and overhead. Moreover, experimental results and theoretical analysis of parameter selection are also provided. We further study the stability and convergence of FNFD theoretically. The study shows that FNFD is always convergent as a control method if and only if the input dataset is persistent exciting.

In the literature, many detection schemes have been proposed to detect NTL frauds. However, some NTL frauds are far more complicated than what the existing schemes expect. We recently discovered a new potential type of frauds, a variant of NTL frauds, called Colluded Non-Technical Loss (CNTL) frauds in the Smart Grid. In a CNTL fraud, multiple fraudsters can co-exist or collaborate to commit the fraud. The existing detection schemes cannot detect CNTL frauds since these methods do not consider the co-existing or collaborating fraudsters, and therefore cannot distinguish one from many fraudsters. In this dissertation, we propose a CNTL fraud detector to detect CNTL frauds. The proposed method can quickly detect a tampered meter based on RLS. After identifying the tampered meter, the proposed scheme can detect different fraudsters using mathematical models. The experiments show that the scheme is effective in detecting CNTL frauds.

The rest of the dissertation is organized as follows. In Chapter 2, we introduce Smart Grid, the background of NTL fraud, and the existing solutions. In Chapter 3, we introduce the first proposed detector, NFD, including the working process, algorithm, experiments and parameter selection. We present the second proposed detector, FNFD, in Chapter 4, which includes the idea and algorithm, as well as the experimental results and

discussion. We present the third detector, CNFD, in Chapter 5. Finally, we conclude the dissertation in Chapter 6.

CHAPTER 2
BACKGROUND AND LITERATURE REVIEW

2.1 Background

The traditional power system distributes electricity from power generation plants to the end consumers in one direction, which is inefficient and unreliable since it cannot satisfy the increasing future demand and the system is lacking efficient monitoring and quick response, easily resulting in power outages. As reported in the paper [48], the cost is approximate 100 billion dollars each year for power outages in US traditional power systems. Smart Grid provides two-way electricity flow and data communication. The two-way electricity flow incorporates distributed renewable energy better, such as solar and wind energy, which benefits both environmental protection and the mitigation of the energy crisis [15]. The two-way data communication provides intensive system monitoring and quick system recovery.

Advanced Metering Infrastructure (AMI) is an automatic pricing, metering and billing infrastructure in Smart Grid which integrates with current state-of-the-art electronic hardware devices and software systems. AMI employs devices including smart meters, relay meters, collectors, charging spots, substations, head-end devices, etc. One or multiple smart meters are installed for each household or business to record energy usage. Relay meters are used to relay messages to other meters or the head-end devices. Collectors are used to gather information in sub-networks. Substations are used to manage electricity distribution and also play a role in managing communication. The head-end devices are servers employed by the utility to communicate with all other devices in AMI.

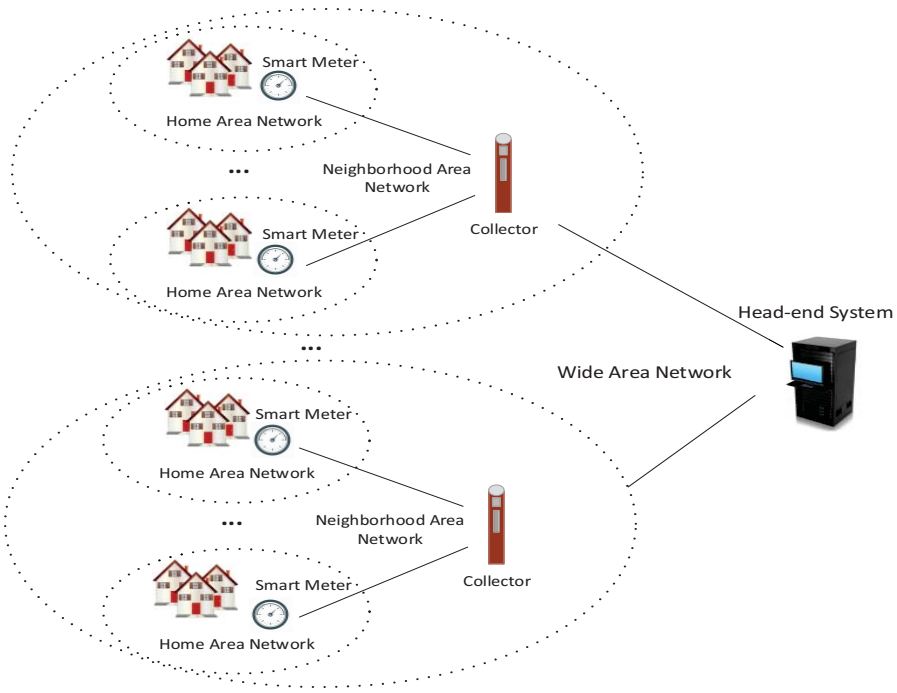

Figure 2.1: The conceptual communication framework of AMI.

Communication in AMI is two way. A smart meter can communicate with any other smart meters in AMI. Each two devices, e.g. smart meters, relay meters, collectors, charging spots, substations, head-end devices, etc. can communicate with each other. As shown in Fig. 2.1, a Home Area Network (HAN) forms when home appliances and smart meters in a household join the AMI. In a community, a collector is installed to gather local information, thus forming a Neighbourhood Area Network (NAN) [60, 62]. When several HANs are connected and report to the head-end systems, it is a Wide Area Network (WAN). In the U.S., the utility employs ANSI C12 serials as the communication protocols for AMI, including ANSI C12.18, 19, 21 and 22 [3].

2.2 Non-Technical Loss Fraud

However, the development of Smart Grid has been raising new security and privacy challenges. Globally, utility companies consistently suffer from NTL frauds. As reported [55], the non-technical loss even exceeds the technical loss in some countries and is

estimated as about 1% of the worldwide electricity consumption. Beside electricity theft, the frauds where customers gain illegal benefit by tampering meters, intruding networks, etc. are also NTL frauds. This silence crime disturbs the normal billing process of power companies, causes money loss, and is a waste of people's efforts on energy conservation. Besides poverty and economy recession, the temptation of free service is another motivation to steal electricity in underdeveloped, developing, and developed countries, not only limited to the low-income population.

The economic loss has been caused by NTL frauds is huge. In developed countries, such as United State, the annual loss is $6 billion [44]. In developing countries, the annual loss due to NTL frauds is $58.7 billion, which is reported in a study of the top 50 emerging market countries, published by northeast group, llc in 2014 [6]. These countries, including China, India, etc., will invest $168 billion to deal with NTL frauds and build reliable Smart Grid till 2034. As Forbes reported [52], Florida utilities lose millions each year, and thousands of NTL frauds have been reported by Duke Energy.

In the traditional power grid, the utility relies on physical methods, such as checking power lines periodically, to detect NTL frauds. In Smart Grid, the development of AMI enables smart meters with the capability of two-way communications. The utility can intensively monitor smart meters to detect NTL frauds remotely. Smart meters dwarf electricity theft using some physical methods, such as bypassing. However, the two-way communication extends adversaries' malicious behavior from the meters to the whole generation, transmission, and distribution process. As FBI reported [56], hacking smart meters is extremely easy and NTL frauds occur in various new forms.

Moreover, privacy protection is another challenge to detect NTL frauds in Smart Grid. Smart meters store energy usage information, and this information are distributed all over the communication networks, which potentially expose customer habits and behaviors [44]. In Smart Grid, the customers lose control over the information delivered to the utility unconsciously. Novel schemes to identify NTL without worrying about privacy

are needed. Furthermore, even if customers are totally willing to provide their personal data, there's still five to ten years before AMI is fully deployed [5]. The utility must find efficient ways to detect NTL frauds right now.

2.3 Problem Definition and Attack Model

A community has N households and charging stations in total, and N smart meters are installed to record the consumption. As shown in Fig. 2.2, the relationship between meters and households or charging stations is one-to-one, and meters are connected to the same secondary distribution network. A utility company is responsible for supplying electricity to this community. However, the utility company found that the total amount of the billing electricity is always much smaller than the amount that it supplied to the community. After having transformers, power lines and other devices examined, the utility company eliminated technical loss. NTL frauds are highly suspected on some meters. The objectives include identifying tampered meters, pinpointing the locations, and learning the behavior of adversaries. The detection processes should be done before the adversaries disappear.

There are two types of adversaries. The first type is the customers who are using these meters. Let's call them inside adversaries. Inside adversaries may have some knowledge of smart meters, thus, they can tamper these meters to lower their electricity bills. Or, they may know nothing about smart meters but they can get hacking tools to tamper meters for free [4]. The second type of adversaries are from the outside. Let's call them outside adversaries. Outside adversaries can manipulate meters remotely or manipulate billing messages in communication networks. They could increase the electricity bills as well as decrease them, but increasing the electricity bills is another type of frauds which is out of the scope. In message manipulation attacks, the meters are intact. However, the adversaries have to intercept the connections between meters and the head-end system to get encryption keys. Therefore, the utility company still has to locate

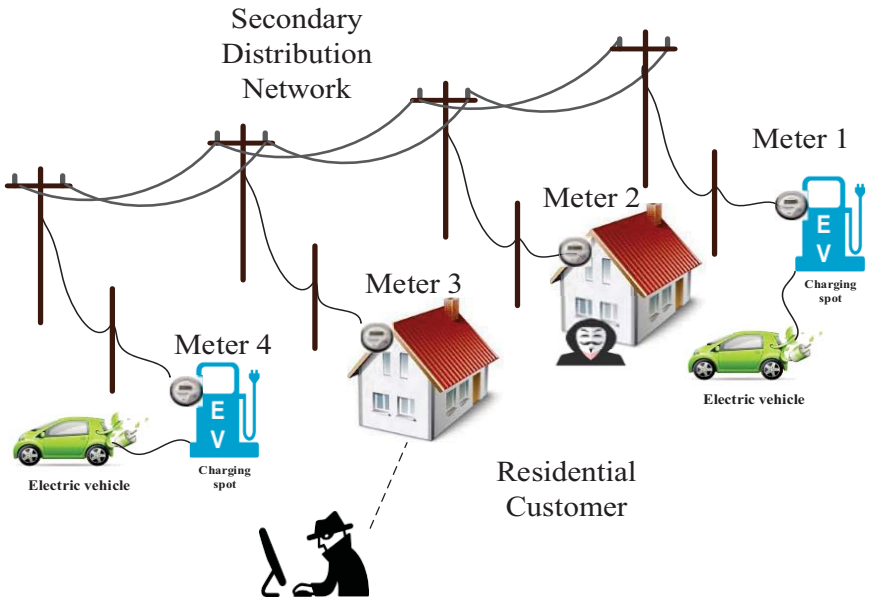

Figure 2.2: The conceptual framework of NTL fraud.

the meters to replace their keys. Under the above consideration, we call a meter as tampered meter when it is either message-manipulated or tampered. The inside adversaries could falsify power consumption and attribute to the neighbors. The prerequisite of this type of attack is the same as message manipulation.

2.4 Literature Review

2.4.1 Physical Method

Physical method is the most direct method to detect NTL frauds. In the traditional power grid, customers get "free" electricity via bypassing a meter. The utility developed a series of physical methods to deal with it including video surveillance, sensor monitoring, human inspection, etc. These methods are still employed in Smart Grid [10, 46, 49, 50, 57]. The paper [50] proposes employing various physical methods including sensor monitoring system, video surveillance system, control system and actuator system. Cameras equipped in drones are used to monitor power lines and report any abnormality. Vigilance staff are needed to examine reported abnormality. These physical methods monitor Smart Grid from

the outside. Correspondingly, some physical methods are used to enhance the reliability from inside the grid. These methods focus on improving the quality of power lines, enhancing the robustness of transformers or employing advanced meters [60, 62]. In the paper [10], Power Line Carrier (PLC) is proposed to install in smart meters. PLC units are responsible for recording the readings of the meters and sending to the PLC host. An NTL fraud can be detected if the readings are different from the readings sent by the meters. However, PLC units have the problem of securing themselves. Typically, physical methods are expensive and inefficient since monitoring devices and human resource are needed.

2.4.2 IDS-based Method

Typical security systems proposed for Smart Grid [27, 37, 41] include AMIDS [45], SCADA [17, 18], and Amilyzer [8]. They are Intrusion Detection Systems (IDS) [33] aiming at general security issues, not designed for detecting NTL frauds. Amilyzer and Supervisory Control and Data Acquisition System (SCADA) both work in AMI to defend various attacks in Smart Grid. Amilyzer is an IDS based on specification. The full name of SCADA is supervisory control and data acquisition system [18]. As its name implies, the function of SCADA is to monitor, interact and control industrial processes and address security issues in these processes. The main purpose of introducing SCADA in Smart Grid is to monitor the generation, transmission and distribution processes preventing potential collapses and outages. They are not introduced to detect NTL frauds. AMIDS claims that it aims at NTL frauds. But it is actually an IDS which functions like Amilyzer. IDS cannot build a relationship between NTL frauds and various attacks.

2.4.3 Profile-based Method

Another typical method employed to detect NTL frauds is user profile analysis, which includes feature extraction, machine learning, data mining, pattern recognition, etc. [9, 12–14]. User profile analysis is based on analyzing the electricity usage of customers and generating profiles for them. Generating profiles requires large volumes of historical data to generalize common features of normal customers, as well as abnormal customers.

The paper [12] employs machine learning to detect NTL frauds. The authors build a knowledge-discovery process to classify customers. At first, a large amount of data in databases are used to extract key features and build profiles. Then, they train a neural network to classify customers based on their features. Fuzzy set is employed in the paper [14] to detect NTL frauds. The first step of the scheme is fuzzy clustering based on C-means. Customers who have similar profiles are classified into the same category. The second step is to build a membership matrix and calculate the Euclidean distances between the centers of the clusters. The third step is to identify abnormal customers and the criterion is a longer distance. Beside data requirement, the drawback of user profile analysis is that it is vulnerable to variations caused by season, weather, travel or some other temporary changes. These variations cause a high false positive rate in methods based on user profile analysis.

2.4.4 Comparison-based Method

Some comparison-based methods are proposed to detect NTL frauds [58, 59, 61]. The basic idea of BCGI [58] is binary coding and code permutation. Smart meters are divided into a few groups, and each meter could be in more than one groups. BCGI employs an inspector for each group. Binary coding is used to code the meters and inspectors with combinations of 1 and 0. When the readings of the inspectors show abnormal, their binary codes are permuted. And the permutation result shows the code of the abnormal meter. However, the weak point of BCGI is that it is not efficient in detecting multiple abnormal meters. And, the number of inspectors needed is nearly half of the number of the meters. Thus, it is not cost-effective. The basic idea of DCI [59] is binary tree pruning. DCI builds a binary tree having the meters as leaf nodes in the tree. Non-leaf nodes are virtual nodes which indicate an inspection on the leaf nodes in the sub-tree. The inspection goes from the root to the leaves pruning normal branches, and finally identify the abnormal node. The weak point of DCI is that it is inefficient dealing with multiple tampered meters, which is similar to BCGI. DCI is built on scanning [61]. In the paper [51], a pole-side meter is

employed, which is similar to an inspector or the observer meter. However, this meter is used to read both the consumption and the supply simultaneously, which is inefficient.

2.4.5 Statistic Method

Generally speaking, statistic method belongs to the family of mathematical method. However, it is usually mentioned seprately. Typical statistic methods used to detect NTL frauds include Optimum-Path Forest (OPF), Bayes' network, decision tree, etc. A Non-cooperative Game (NCG) model is built to detect NTL frauds in the paper [40]. The idea behind NCG model is decision-making and the probability of different behaviors, including normal behavior, likely fraud behavior and serious fraud behavior. The basic idea of the paper [35] is probability-driven state estimation. Firstly, it estimates the loads of distribution transformers, which is based on the aggregated meter readings. Then, some customers are suspected after analyzing the variances between estimations and the real values. Statistic methods mimic the decision-making process of maintenance specialists. Nevertheless, the decision-making of human is not simply based on a larger probability.

CHAPTER 3

NFD: NTL FRAUD DETECTION

3.1 Introduction

In this chapter, we propose a novel detector, named NFD (NTL Fraud Detection) [26, 31], to detect NTL frauds in Smart Grid. No additional software products are required to install on either side of Smart Grid. The detector does not require personal data, such as electricity consumption of each appliance in 24×7 hours to analyze user behaviors, but a central observer meter for a group of consumers under investigation. This observer meter is responsible for recording the total amount of power supplied to a group during a certain time duration. Based on these data and billing electricity of each meter, we obtain mathematical models of tampered meters and normal meters according to their different characteristics which can identify meters with NTL frauds.

Not only NFD can detect a single meter tampered by a single adversary, but also, it can detect multiple meters tampered by multiple adversaries. NFD is based on Lagrange polynomial to model an adversary's behavior, and detect a tampered meter by comparing the difference between the results. Different adversaries have different behaviors. By modeling the behaviors of adversaries, NFD can identify multiple meters tampered by multiple adversaries. With these models, NFD even knows adversaries better than adversaries themselves. The proposed detector can solve the NTL fraud problem in both Smart Grid and the traditional power grid.

3.2 Working Process and Algorithm

NFD needs an additional device installed to record the total electricity supplied to n meters under its observation, which we call it an observer meter. In fact, at the most of the cases, such an observer meter already exist, called a head meter, e.g., in an apartment building. After further investigation, n meters are highly suspected by the utility. Thus, we install a central observer meter in the same secondary distribution network with these meters, shown in Fig. 3.1. This observer is responsible for recording the total amount of electricity supplied to the group of n ($n \leq N$) meters. This observer is installed outdoor and with a distance to the households since we are not allowed to observe the customers closely due to the privacy concern. Moreover, the data collected are only the usage data that the customers should provide for billing.

To introduce NFD, we first introduce some notations. Let's denote the j-th measured time duration as T_j. During T_j, the total amount of electricity recorded by the observer is denoted as E_j. During T_j, the amount of electricity consumed by a household i is denoted as $E_{i,j}$. However, the billing amount may be a different value from $E_{i,j}$. Let's denote the billing amount as $x_{i,j}$, which is recorded by Meter i during T_j. Here, $1 \leq i \leq n$ and $1 \leq j \leq m$. For convenience and diversity, we use three terms changeable, and they are "electricity measured", "electricity registered" and "electricity reported" .

For a normal meter, the amount of electricity consumed by the household and the amount registered by this meter should be the same, which means $E_{i,j}/x_{i,j} = 1$. However, there exist measurement errors. If considering measurement accuracy, $|E_{i,j}/x_{i,j} - 1|$ should be very small. Let's define an accuracy ratio $\alpha_{i,j}$, which is denoted as:

$$\alpha_{i,j} = E_{i,j}/x_{i,j}, \tag{3.1}$$

to represent the error of Meter i in the time duration j.

We define a value range for $\alpha_{i,j}$ as $[\alpha_{min}, \alpha_{max}]$. Thus, we can define a meter as

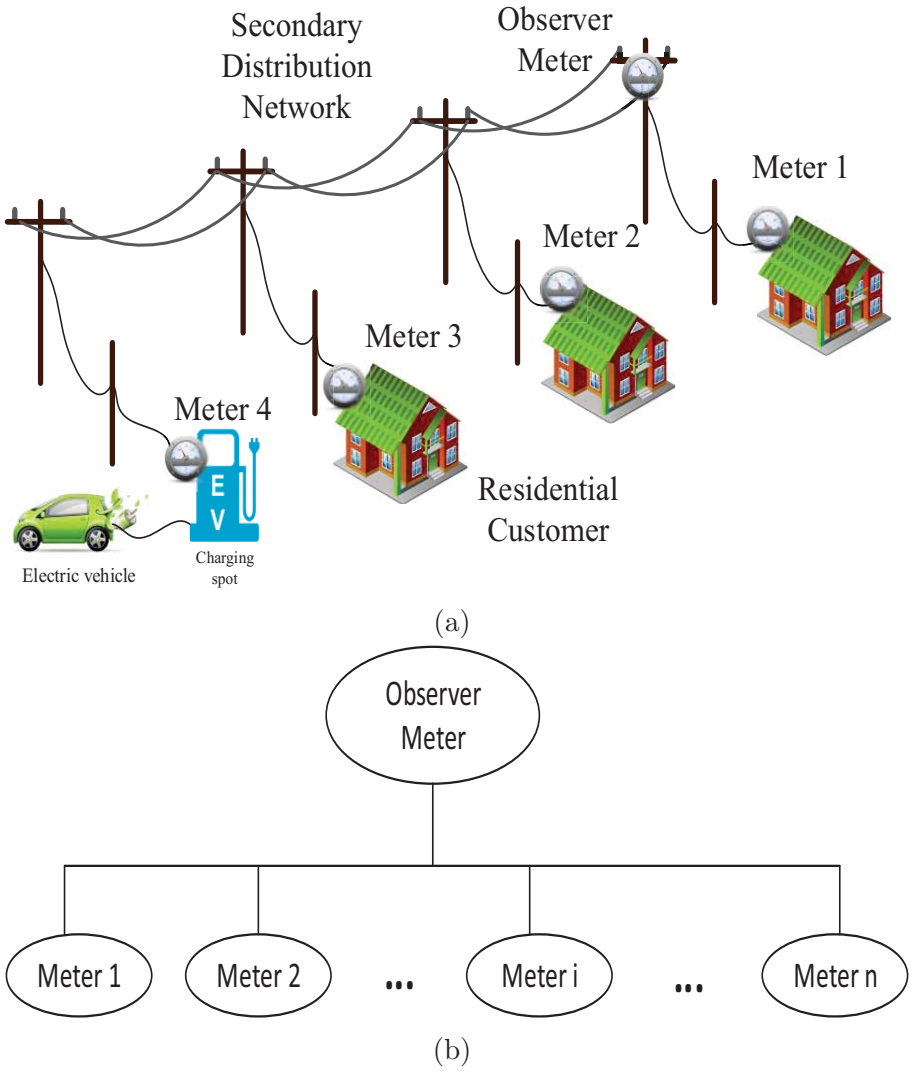

Figure 3.1: Install an observer meter. a) An observer meter is installed along the pole side in a community and it records the supply to several suspected meters. These meters are either connected to a household or a charging station for electric vehicles. b) This is the simplified model of the metering system.

normal when $\alpha_{i,j} \in [\alpha_{min}, \alpha_{max}]$, where $1 \leq i \leq n$ and $1 \leq j \leq m$. A typical value of α_{min} is 0.98 and a typical value of α_{max} is 1.02. Moreover, we can also believe that a meter is tampered when $\alpha_{i,j} > \alpha_{max}$. Each meter may have different accuracy, but the difference is slight. We assume that all the meters have the same accuracy for simplicity.

$(x_{i,j}, i = 1, 2, \cdots, n)$ are a series of the values of the billing electricity, and their values are available. However, we do not know the values of $(E_{i,j}, i = 1, 2, \cdots, n)$. Thus, we cannot identify the tampered meters only by the comparison between $x_{i,j}$ and $E_{i,j}$. We notice that there is a point at the coordinate for each value pair $(x_{i,j}, E_{i,j})$, shown in Fig. 3.2. For Meter i, there are a group of value pairs related to it, and we can use the following function to represent these points:

$$y_i = f_i(x), \ where \ f_i(x_{i,j}) = E_{i,j}, j = 1, 2, \cdots, m. \tag{3.2}$$

where that $f_i(x)$ stands for the behavior function of meter i and is what we need to figure out.

Under the above assumptions, we have the following corollary, where the proof is easy, and thus is omitted.

Corollary 3.1. *For Meter i, it is a tampered meter, if and only if its curve, $f_i(x)$, is above the line of $f(x) = \alpha_{max}x$.*

Corollary 3.1 can be illustrated in Fig. 3.2. The curve of $f_5(x)$ is between the lines of $f_1(x) = \alpha_{max}x$ and $f_6(x) = \alpha_{min}x$, and it is regarded as a normal meter. When the curves, such as the curves of $f_2(x)$, $f_3(x)$ and $f_4(x)$, are above the line of $f_1(x) = \alpha_{max}x$, their corresponding meters are regarded as tampered. Each point on the coordinate of Fig. 3.2 is the value pair, (*the measured electricity*, *the consumed electricity*), of each meter. The functions of these curves could be

- $f(x) = ax + b$, where a and b are two constants, $a > \alpha_{max}, b \geq 0$;
- $f(x) = x^u$, where u is a constant;

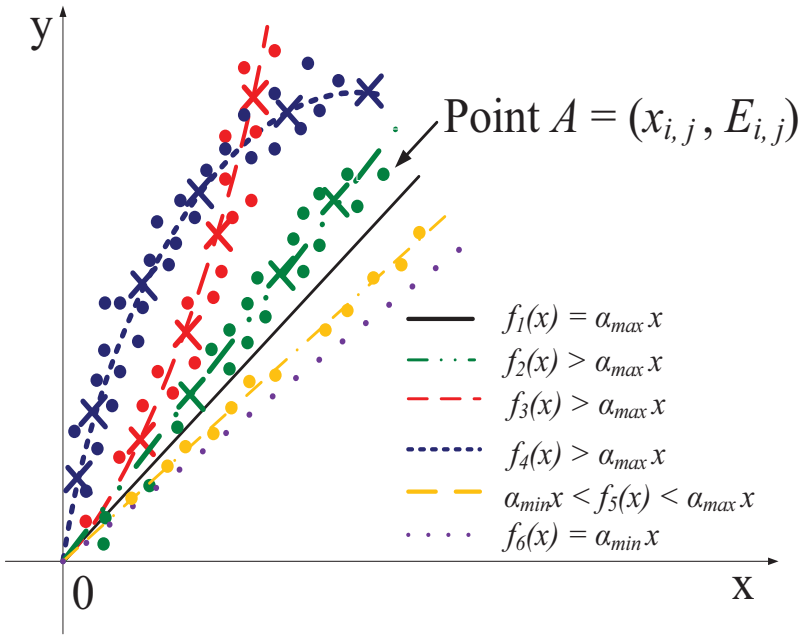

Figure 3.2: Points on the coordinate, with the corresponding value pairs (the measured electricity, the consumed electricity). Curves of the normal meter and the possibly tampered ones. The black line is of the normal meter. Other curves above this line are different potential curves of the tampered meters according to Corollary 3.1.

- $f(x) = a^x$, where a is a constant and $a > 0, a \neq 1$;
- $f(x) = a\sin(bx + c)$, where a, b, and c are three constants, and $a > 0$;
- $f(x) = a\arcsin(bx + c)$, where a, b, and c are three constants, and $a > 0$;
- Other functions $f(x) > \alpha_{max}x$.

Algorithm 1 On-line NFD: NTL fraud detection

```
Initiation: choose n from N, choose initial m and m_max, set l = 0
for Each observer meter j do
   On_Timer:
   each meter records observed value and registered value
   l ← l + 1
   if l = mn then
      calculate [X] and [E_T]
   check linear independence of [X] and [E_T]
   if not linear independent then
      replace the last record with new measurement
   else
      kill timer
   calculate and normalize [A]
   obtain polynomial f_i(x) of each meter i
   for each f_i(x) do
      if f_i(x) > α_max x then
         identified as tampered
      if α_min x ≤ f_i(x) ≤ α_max x then
         identified as normal
      else
         try a larger m
         break
```

Based on Lagrange polynomials, if we have $m + 1$ samples, $(x_{i,j}, E_{i,j}), 0 \leq j \leq m$, we can find an approximation function to represent them, and this function can be written as follows:

$$f_i(x) = \sum_{k=m}^{0} a_{k,i}x^k, \tag{3.3}$$

where $a_{k,i}$ is the coefficients and $f_i(x_{i,j}) = E_{i,j}$.

If we know the values of the $m + 1$ samples, we can obtain the coefficients $(a_{k,i})$ by direct calculation, and thus, get the function of Meter i using Eq. (3.3). But, till now we

only get to know the values of $(x_{i,j}, j = 1, 2, \cdots, m)$ and we do not know the values of $(E_{i,j}, j = 0, 1, \cdots, m)$.

Since the distance between the observer and the meters under observation is not long, the technical loss is small enough to ignore. Under this assumption, to obtain the coefficients $(a_{k,i})$, E_j can be written as:

$$E_j = \sum_{i=1}^{n} E_{i,j}. \tag{3.4}$$

Moreover, E_j, the summation of $E_{i,j}$ is available. Then, we have the following summation: $E_j = \sum_{i=1}^{n} E_{i,j} = \sum_{i=1}^{n} f_i(x_{i,j}) = \sum_{i=1}^{n} \sum_{k=m}^{0} a_{k,i} x_{i,j}^k$.

We notice that when the amount of the billing electricity is zero, the amount of consumed electricity must be zero as well. Thus, in Eq. 3.3, $a_{0,i}$ should be zero. We adjust the range of k to $[1, m]$. Furthermore, we re-write Eq. 3.4 as follows:

$$E_j = \sum_{i=1}^{n} \sum_{k=m}^{1} a_{k,i} x_{i,j}^k. \tag{3.5}$$

Now, the values of $x_{i,j}$ are available in Eq. (3.5), as well as the values of E_j. The values of all coefficients $a_{k,i}$ are unknown. Since there are n meters and m measurements, the total number of $a_{k,i}$ is $n \times m$.

Let's denote the array of the values of E_j as E_T. Let's denote the array of all coefficients as A. Moreover, we use X to represent the matrix of the measurements. Then, we have:

$$E_T = (E_1, E_2, \cdots, E_m)^T, \tag{3.6}$$

$$
\begin{aligned}
A = (&a_{m,1}, \ldots, a_{k,1,}, \ldots, a_{1,1}, a_{0,1}, \ldots, \\
&a_{m,i}, \ldots, a_{k,i}, \ldots, a_{1,i}, a_{0,i}, \ldots, \\
&a_{m,n,} \ldots, a_{k,n}, \ldots, a_{1,n}, a_{0,n}) \,,
\end{aligned} \tag{3.7}
$$

$$
X = \begin{pmatrix}
x_{1,1}^{m} & \ldots & x_{1,1}^{k} & \ldots & x_{n,1} & 1 \\
x_{1,2}^{m} & \ldots & x_{1,2}^{k} & \ldots & x_{n,2} & 1 \\
\vdots & \vdots & \vdots & \vdots & \vdots & \vdots \\
x_{1,j}^{m} & \ldots & x_{1,j}^{k} & \ldots & x_{n,j} & 1 \\
\vdots & \vdots & \vdots & \vdots & \vdots & \vdots \\
x_{1,nm}^{m} & \ldots & x_{1,nm}^{k} & \ldots & x_{n,nm} & 1
\end{pmatrix}, \tag{3.8}
$$

$$
E_T = X \times A, \tag{3.9}
$$

$$
A = X^{-1} \times E_T. \tag{3.10}
$$

The values of E_T and X are available from the data of each measurement. Moreover, we can obtain the values of X^{-1} by matrix inverse of X. Now, from Eq. (3.10), we get all of the coefficients. One constraint of the $n \times m$ equations is that they should be linearly independent. We can get all the polynomials by putting the coefficients into Eq. (3.3). For each meter, there exists a polynomial to represent it. By analyzing the relationship between a polynomial and $f(x) = \alpha_{max}x$, we can identify the tampered meters. If the curve of a polynomial is above the line of $f(x) = \alpha_{max}x$ at the coordinate, the related meter is identified as tampered. If the curve of a polynomial is between the lines of $f(x) = \alpha_{max}x$ and $f(x) = \alpha_{min}x$, the related meter is identified as normal. If there is any curve of a polynomial is under the line of $f(x) = \alpha_{min}x$, the detection process should report an error.

We aim to detect meters which are tampered on purpose to gain illegal benefits.

Thus, for each meter, its billing electricity is less than or equals to the amount of electricity consumed. Colluding attacks occur when adversaries compromise a meter so that the customer has to pay more than (s)he consumed. This problem is not what we want to solve here, but it is our current research.

The proposed NFD algorithm can be used both on-line and off-line. For the off-line detection, we need to identify NTL frauds out of a certain given dataset. Since the number (n) of meters and the times of measurements are already known in the dataset, what we need is to choose an appropriate order m, where $m \leq the\ times\ of\ measurements$. For the on-line detection, we need to gather data from each measurement and identify frauds real time. The on-line detection algorithm can be seen in Alg. 1. It will choose an initial order m and then keep gathering data until it gets enough data to build an independent matrix. If the initial m is not satisfying, it will try a higher m and repeat the whole process until it reaches either of the following two conditions:

1. Condition 1: every meter is identified as either tampered or normal;
2. Condition 2: $m \geq m_{max}$ and m_{max} is the maximum value of the desired order m.

The main steps of the detection process include preparation, calculation, normalization, and comparison. In the first step, parameters are chosen to initialize the process. In the second step, coefficients are obtained according to Alg. 1. In the third step, the results are normalized. In the final step, we compare the polynomials with $f(x) = \alpha_{max}x$ to identify tampered meters.

We discuss parameter selection in details in Section 3.4.

3.3 Experiments

We conducted various experiments to test NFD, and some of the experiments are introduced in this section. We use kWh as the unit for electricity values listed in the tables. The data used in our experiments are simulated. According to a report [2], the

average household electricity usage around the world varies from 570 kWh to 11879 kWh in 2010. The experimental data are randomly generated within this range. We manually altered some meters' usage data letting the billing amount less than the original (consumed) amount.

3.3.1 Experiment 1: No Tampered Meters

In this experiment, the dataset contains the data of 10 meter and an observer. We list the data of 20 measurements, including the amount of the billing electricity and the amount of the recorded value of the observer, shown in Table 3.1.

Table 3.1: The unit of the billed electricity (kWh) of 10 meters and an observer meter in NFD - Exp. 1

Meter 1	2	3	4	5	6	7	8	9	10	Observer
4560	3300	6780	1900	2870	3200	4510	2800	4320	5100	39340
5120	2560	4560	2440	1900	4500	5700	2120	5700	6700	41300
3230	3500	6780	3900	1670	5100	4340	2000	5200	6400	42120
6780	2900	5990	1890	2560	6700	5800	5300	6880	6890	51690
6430	3000	5300	2120	4980	7450	6400	3050	4990	4800	48520
1670	4300	5440	2800	5880	4560	6340	3560	4670	5120	44340
2430	2700	6330	3000	2200	1400	5300	3650	4770	5700	37480
7890	2300	4600	1900	2560	5700	4670	3670	2120	1440	36850
8700	3400	6120	2650	2780	6120	6400	3100	5670	5870	50810
4400	1400	3670	2990	2330	1670	4600	3540	5600	4660	34860
5200	2800	4780	2110	5430	3120	5600	3000	5900	4670	42610
3560	2900	5340	2440	5280	4230	5670	2890	4900	4220	41430
2450	4500	5200	2660	3760	5230	5800	2400	2220	2780	37000
4560	3890	5780	2770	4670	5400	6200	2670	3450	3990	43280
3670	2700	6400	3120	4980	6400	6900	2670	3560	6450	46850
3560	4100	5990	3450	4330	4780	6770	1990	4110	5980	45060
2340	3330	6900	3200	3780	1560	5440	2500	4560	5840	39450
5320	3990	5550	3320	4550	9530	6780	5700	4880	6330	55950
3240	3980	5090	1990	2670	4500	7000	3890	4670	5300	42330
4670	2900	4200	2550	4670	8670	7100	3600	5450	8120	51930

In this experiment, we use the Lagrange polynomial with order 2. Since the dataset only contains the data of 20 measurements, we cannot use an order higher than 2.

Moreover, the polynomial is as follows:

$$f_i(x) = a_{2,i}x^2 + a_{1,i}x. \tag{3.11}$$

Based on Eq. (3.10), we can get the values of A. After calculation and normalization, we get

$$A = (0, 1, 0, 1, 0, 1, 0, 1, 0, 1, 0, 1, 0, 1, 0, 1, 0, 1, 0, 1).$$

The obtained polynomials of all meters are shown in the second column of Table 3.2. We compare the polynomials with $f(x) = \alpha_{max}x$ and find that none of the meters are tampered. In other words, there are all normal meters.

Table 3.2: The results of the experiments: the polynomials of all meters. There are 10 meters in Experiments 1 and 2, respectively, and 4 meters in Experiment 3.

No.	Experiment 1	Experiment 2	Experiment 3	Lowering order
1	$f_1(x) = x$	$f_1(x) = x$	$f_1(x) = 0.1x^2 + x$	$f_1(x) = -0.265x^2 + 1.308x$
2	$f_2(x) = x$	$f_2(x) = x$	$f_2(x) = 0.5x^2 + 0.3x$	$f_2(x) = 1.123x^2 - 6.308x$
3	$f_3(x) = x$	$f_3(x) = x$	$f_3(x) = 0.1x^2 + 0.9x$	$f_3(x) = 0.006x^2 + 0.265x$
4	$f_4(x) = x$	$f_4(x) = x$	$f_4(x) = 0.3x^2 + x$	$f_4(x) = 0.458x^2 - 1.681x$
5	$f_5(x) = x$	$f_5(x) = x$	N/A	$f_5(x) = -0.004x^2 + 0.845x$
6	$f_6(x) = x$	$f_6(x) = x$	N/A	$f_6(x) = -0.338x^2 + 6.128x$
7	$f_7(x) = x$	$f_7(x) = 0.1x^3 + 0.5x^2 + x$	N/A	$f_7(x) = 1.8x^2 - 3.32x$
8	$f_8(x) = x$	$f_8(x) = x$	N/A	$f_8(x) = -0.42x^2 + 3.32x$
9	$f_9(x) = x$	$f_9(x) = x$	N/A	$f_9(x) = -0.21x^2 - 0.41x$
10	$f_{10}(x) = x$	$f_{10}(x) = x$	N/A	$f_{10}(x) = 0.11x^2 + 0.364x$

3.3.2 Experiment 2: Single Adversary and Single Tampered Meter

In this experiment, the dataset contains the data of 10 meters and an observer. Table 3.3 shows the values of the amount of the billing electricity and the amount of the supplied electricity recorded by the observer in 30 measurements.

In this experiment, we employ the polynomial with an order of 3, which is as follows:

$$f_i(x) = a_{3,i}x^3 + a_{2,i}x^2 + a_{1,i}x. \tag{3.12}$$

Table 3.3: The unit of the billed electricity (kWh) of 10 meters and an observer meter in NFD - Exp. 2

Meter 1	2	3	4	5	6	7	8	9	10	Observer
2110	3300	4710	1500	3000	8230	4500	2800	4600	5300	59287.5
1950	2600	5330	2330	1530	8550	5600	4494	5100	5600	73951.6
1800	3500	6600	2560	1990	9000	4800	2000	5200	6100	66129.2
2220	2900	6780	1890	2560	9980	5120	5000	6780	6990	76749
2300	3000	4990	2120	4560	8770	6000	3050	4900	4670	83960
1570	3700	6100	2890	5660	8990	6340	3500	4880	5120	94331.8
2500	2700	6230	3000	2200	7990	5300	3600	4780	5330	72562.7
2300	3200	4780	1900	2560	8230	4990	3670	2100	5900	64505.2
2880	3400	5330	2440	2890	8450	4890	3090	5800	5810	68629.1
1930	3100	3550	2670	2330	8650	4600	3550	5700	4890	61283.6
2120	2500	4880	2110	5330	8100	4500	2990	5550	4550	61867.5
2300	2900	4940	2230	5280	7450	5670	2890	4900	4200	77062.9
2000	2900	5120	2660	3600	7810	5800	2700	2100	2600	736212
1750	4000	5440	1990	4670	9110	6200	2560	3600	3900	86272.8
1820	2700	5980	3120	4880	9300	6900	2670	3700	6230	103955.9
2740	2760	5770	3450	4330	8560	6770	1900	4100	6430	100755.3
2450	3330	4890	3330	3990	8440	5440	2500	4800	5810	75875.7
2530	3670	5220	3320	4550	9400	6450	3060	4900	6300	97034.9
2320	3980	5540	1970	2550	9910	6340	3560	4780	5900	92431.8
2780	2990	5900	2550	3890	8760	6100	3880	5600	5660	89413.1
2300	3450	6780	1770	3200	7770	5990	3660	1200	1900	77452.2
3450	4320	7120	1800	3560	7650	5870	3400	1340	1980	77944.7
5320	2450	8120	2890	4120	8010	5770	3080	2450	200	78266.5
4340	3090	7890	3120	4030	7990	5050	2090	2980	4500	70710
2630	4670	6120	3450	2120	7120	6120	4090	2100	5230	85299.3
3120	5120	6660	3200	2670	6890	4890	3900	3210	6120	69429.1
3090	3100	6450	4300	3400	6770	4990	3890	4500	5900	71265.2
1980	3980	5700	3780	3080	6080	5340	3100	4090	4980	71595.1
2890	4560	7230	3880	3030	6130	5220	2030	1900	4870	69587.9
2770	3900	7450	3200	3980	7450	5090	2450	2890	800	66121.3

Using Eq. (3.10), the values of A can be obtained. The results after normalization are as follows:

$$A = (0, 0, 1, 0, 0, 1, 0, 0, 1, 0, 0, 1, 0, 0, 1,$$

$$0, 0, 1, 0.1, 0.5, 1, 0, 0, 1, 0, 0, 1, 0, 0, 1).$$

The polynomials of all the 10 meters in this experiments are shown in the third column of Table 3.2. The curves of meters are shown in Fig. 3.3. After comparing between these polynomials and $f(x) = \alpha_{max}x$, we notice that the curve of the 7^{th} meter is above the line of $f(x) = \alpha_{max}x$. Thus, the 7^{th} meter is a tampered meter.

3.3.3 Experiment 3: Multiple Adversaries and Multiple Tampered Meters

In this experiment, the dataset contains the data of 4 meters and an observer. The amount of the billing electricity and the amount of the supplied electricity in 8 measurements are listed in Table 3.4. We employ the polynomial with an order of 2, which is the same as in Exp. 1.

Table 3.4: The unit of the billed electricity (kWh) of 4 meters and an observer meter in NFD - Exp. 3

Meter 1	Meter 2	Meter 3	Meter 4	Observer Meter
2100	4000	3000	6700	35508
1800	5000	4000	10300	63451
2500	3600	8000	4500	34860
1900	5300	6000	5600	41904
2200	6300	7000	8900	68282
2600	4000	4500	9400	54459
3000	5000	3400	8700	53523
1700	3000	3700	8600	42876

Now we can obtain A, according to Eq. (3.10). After calculation and normalization, we get

$$A = (0.1, 1, 0.5, 0.3, 0.1, 0.9, 0.3, 1).$$

The obtained polynomials of all the meters in this experiment can be seen in the fourth column of Table 3.2. After comparing these polynomials with $f(x) = \alpha_{max}x$, we find

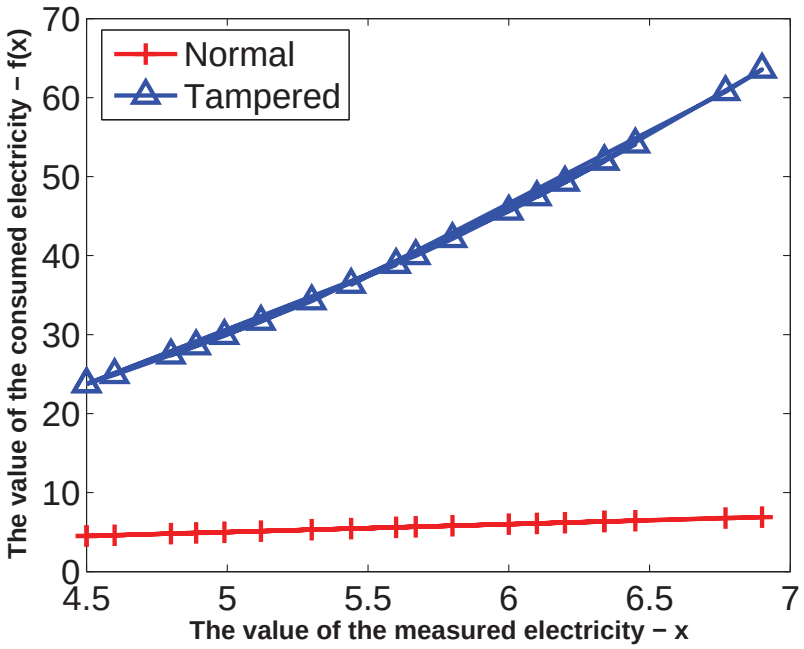

(a)

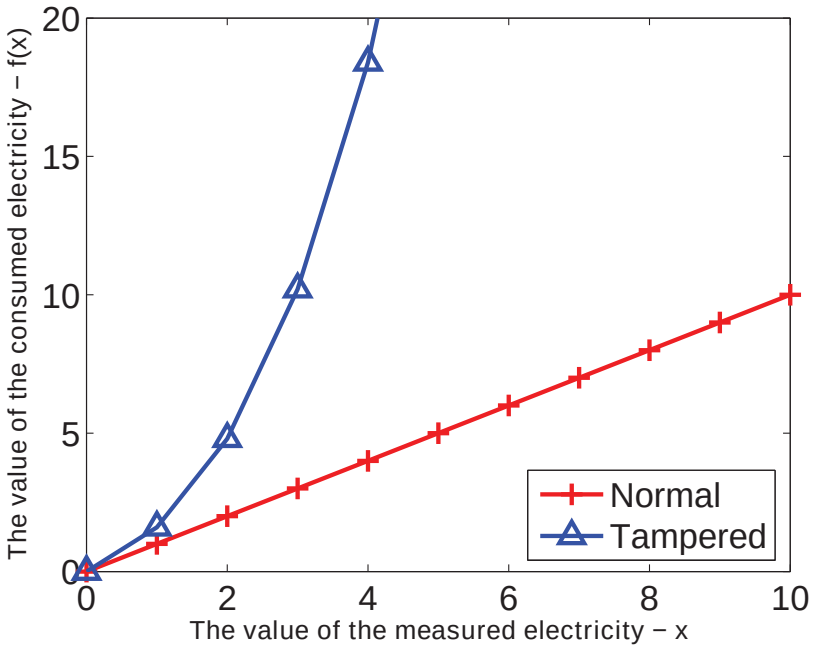

(b)

Figure 3.3: The curves of all the polynomials in Experiment 2. The range of x shown in a)is obtained from the related dataset. The range of x in b)is extended to [0,10].

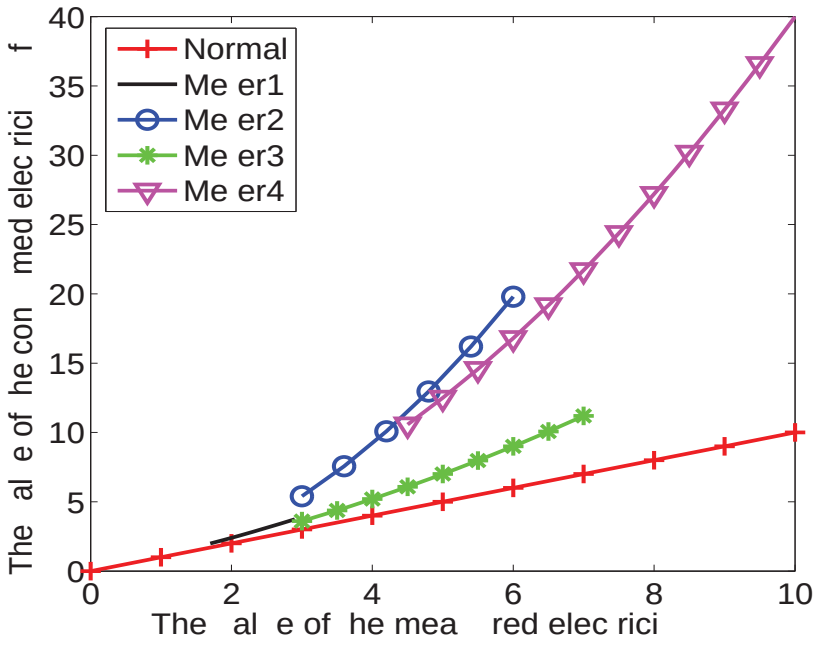

(a)

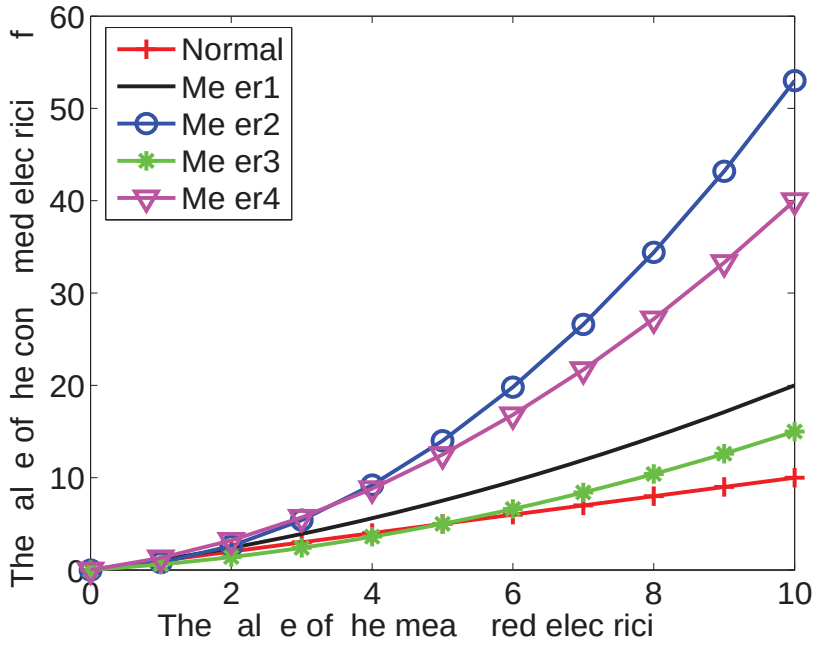

(b)

Figure 3.4: The curves of all the polynomials in Experiment 3. The range of x shown in a)is obtained from the related dataset. The range of x in b)is extended to [0,10].

that all the meters are tampered meters. The curves of these meters, with a comparison to the normal meter, are shown in Fig. 3.4.

3.4 Parameter Selection and Discussion

The selection of the order m is decided by accuracy requirement. If a higher accuracy is required, a bigger m is needed, at the most of the time. Also, more measurement data are needed to obtain a polynomial with a higher order of m. However, a bigger m not always results in a higher accuracy.

In this section, some discussions will be carried out to guide applicable usage of this scheme. Theoretical analysis and related proofs will be carried out, together with some case studies. Its main purpose is to answer the following questions:

- How to choose the order m?
- For a given order m, what should the error be?
- To lower the error, should we choose a higher m?
- For a given order m, how many measurement data do we need?
- How many meters should be in the same group (how to choose n)?
- How much detection time is needed to identify a fraud?
- How many observer meters are needed in a community?

3.4.1 Error and Selection of Order m

In this subsection, we'll discuss the relationship between the order m and the corresponding error. Related theoretical analysis and case study will help to choose a better value of the order m.

Now, we'll use the same dataset in Experiment 2 to illustrate the error. In Experiment 2, we use an order 3 polynomial to fit the dataset. Here, we try to use an order 2 polynomial to fit the dataset. The result is shown in Table 3.2.

From Table 3.2, the last column, maybe it is hard to identify the tampered one. But it is easy to differentiate the tampered meter from those normal meters in Fig. 3.5. The black line is the normal meter with the polynomial of $f(x) = \alpha_{max}x$. The lines or curves above this black one are suspected to be tampered. We can see that only the curves of Meter 6 and Meter 7 are above it. Moreover, for Meter 6, its slope rate is almost the same as the normal meter. Meter 7's curve is far from the normal one with a sharper slope. Meter 7 is tampered, as the result of Experiment 2. But for Meter 6, it is a false alarm. The reason is that to get the order 2 polynomial, we only need 20 out of the total 30 measurements dataset in Experiment 2. The occurrence of error is caused by lower accuracy. Reversely, to identify the tampered meters accurately, more data or measurements are needed.

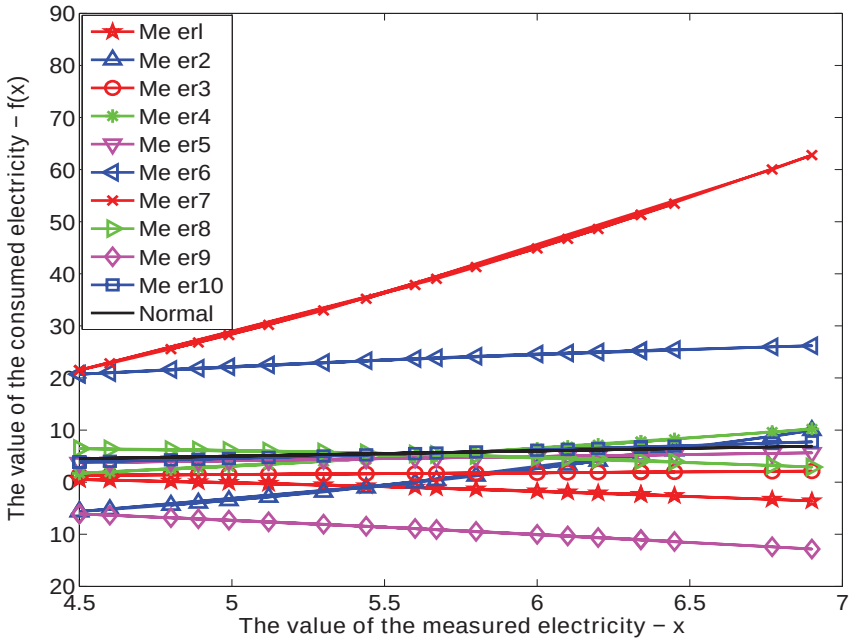

Figure 3.5: The curves of the polynomials in the experiment of lowering order. A false alarm occurs when using an order-2 polynomial instead of an order-3 polynomial.

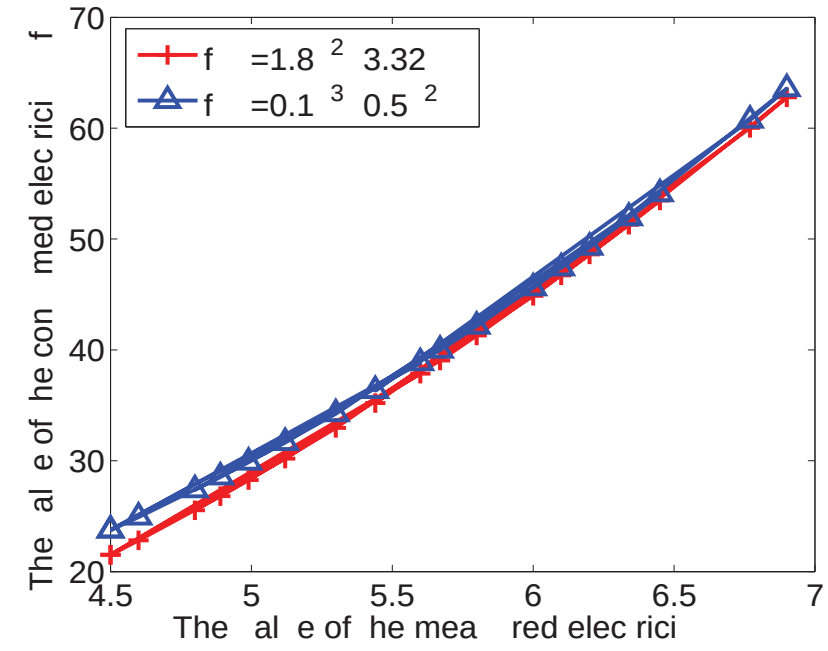

(a)

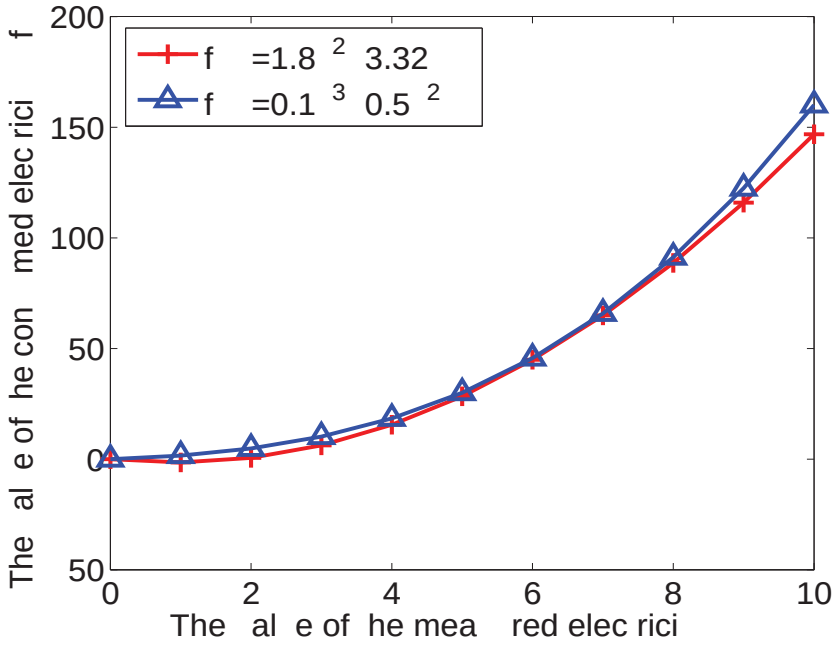

(b)

Figure 3.6: Error comparison between the order 2 and order 3 polynomials of the same meter - Meter 7, obtained from the same dataset in the experiment. The range of x shown in a)is obtained from the related dataset. The range of x in b)is extended to [0,10].

The comparison of the order 2 and order 3 curves of the same meter - Meter 7, is shown in Figs. 3.6(a) and (b). The range of x in Fig. 3.6(a) is the same as in the experimental dataset. Fig. 3.6(b) shows the curves where x is in $[0, 10]$.

The error between the approximation polynomial and its original function, according to Lagrange remainder theorem [54], can be given as:

$$R_n(x) = \frac{f^{n+1}(\xi)}{(n+1)!}(x - x_0)^{n+1}, \xi \in [x_0, x]. \tag{3.13}$$

However, we cannot get to know the original form of the function only from two of its approximation polynomials. Here, we propose another method, to estimate the error of lowering order. Let's define:

e is the error of lowering the order;

x_i is the value of the measured electricity in each Meter i;

$f_1(x_i)$ is the corresponding value of x_i in the lower-order polynomial $f_1(x)$;

$f_2(x_i)$ is the corresponding value of x_i in the higher-order polynomial $f_2(x)$;

n is the number of sample points obtained from each of the polynomials.

Definition 3.1. *Assume that a meter has two polynomials, $f_1(x)$ and $f_2(x)$, which are obtained from the same dataset of measurements, where $f_2(x)$ is the higher-order polynomial and $f_1(x)$ is the lower-order polynomial. Their relative error is given by:*

$$e = \sqrt{\frac{\sum\limits_{x_i=x_1}^{x_n} \left(\frac{f_1(x_i) - f_2(x_i)}{f_1(x_i)}\right)^2}{n}}. \tag{3.14}$$

Conjecture 3.1. *The error - e given in Definition 3.1 can describe the relative error of two polynomials with different orders obtained from the same dataset. Its accuracy is in the same order of magnitude of Lagrange remainder as given in Eq.* (3.13).

Now consider the function $f(x) = 2\sin(x)$. Its Taylor approximation, when $x_0 = 0$, is as follows:

- Order-1: $f(x) = 2x$;
- Order-2: $f(x) = 2x$;
- Order-3: $f(x) = 2x - 1/3x^3$;
- Order-4: $f(x) = 2x - 1/3x^3$;
- Order-5: $f(x) = 2x - 1/3x^3 + 1/60x^5$.

Table 3.5: Comparison of the accuracy magnitude between our definition and Lagrange remainder

Operation	Our Definition	Taylor	Accuracy Mag.
Order 3 $\rightarrow$ order 2	e = 0.29	e = 0.13	10^{-1}
Order 5 $\rightarrow$ order 4	e = 0.028	e = 0.014	10^{-2}

We calculate the relative error according to Eq. (3.14) and Eq. (3.13). Note that in Eq. (3.13), we set $x_0 = 0$, and calculate its relative error. For example, the relative error of the order 5 and the order 4 is $R_5(x) - R_4(x)$. From the result shown in Table 3.5, their accuracies are in the same order of magnitude. Although we cannot prove it now, since we do not know the original form of the function, this conjecture still can guide some practical usage of the scheme. According to Eq. (3.14), the error in our experiment of lowering the order is 4%.

Thus for a certain amount of given datasets (for off-line detection), how to determine the order of the polynomial needed to identify a fraud? Based on the results of Experiment 3, most people may believe to get the most accurate polynomial, the best is to use the whole dataset of all measurements. That is

$$m = \lfloor (l/n) \rfloor. \tag{3.15}$$

However, a higher order m does not result in a higher accuracy sometimes. Now suppose that:

- The number of meters is n;
- The total time of measurements is l, only refer to the measurements with complete data;
- The needed order of the polynomial is m.

Theorem 3.1. *Obtaining more measurements or using a larger historical dataset to obtain a polynomial with a higher order does not always improve the accuracy of the polynomial.*

Proof. see Appendix A. □

Theorem 3.1 tells us that a higher order m does not always increase the detection accuracy. In Theorem 3.1, we present two lemmas. Lemma A.1 tells us when a higher order m can increase the detection accuracy, and Lemma A.2 tells us when a higher order m cannot increase the detection accuracy.

Under some circumstances, if the dataset is too large, we need to choose a subset of the data measured, and to get a relatively lower but good m. The criterion that we propose is to constrain the error - e, as in Eq. (3.14), within the accuracy class. That is

$$e < |\alpha - 1| . \tag{3.16}$$

Under some circumstances, if the dataset is too small for more accurate analysis, or we need a shorter detection time, we can ignore some coefficients, to get a better result with limited data.

Lemma 3.1. *With limited data gathered, ignoring a_0 can improve accuracy and save detection time. That is: when $l \leq 3n$, where l is the number of measurements with complete data gathered,*

$$f_i(x) = a_{m,i}x^m + a_{m-1,i}x^{m-1} + \cdots + a_{k,i}x^k + \cdots + a_{1,i}x. \tag{3.17}$$

Proof. Compare it to Eq. (3.3). For n meters, Eq. (3.17) needs n fewer times of measurements to get the result so that it will save detection time. Moreover, based on the same dataset, with Eq. (3.17) we can get one order higher than with Eq. (3.3). According to Lemma A.1 (see Appendix A), with Eq. (3.17), we can get a higher accuracy. Note that the situation mentioned in Lemma A.2 (see Appendix A), only occurs in high order approximation, rather than ≤ 5 order. □

For most on-line cases, m can be chosen as 2 initially, and according to Alg. 1, m can be adjusted to a higher order towards m_{max}. In most off-line cases, m_{max} can be chosen as 3 to 5, according to different sizes of datasets. Typically, an order of $m_{max} = 5$ is enough for most practical applications.

3.4.2 Detection Time and Selection of User Number n

In this subsection, we will discuss fraud detection time, how to select n out of the total N users or meters in a community, and the number of observer meters needed.

The detection time t is decided by the desired order m, the number of meters under observation n, and the time interval of measurement T_0. It's given as

$$t = mnT_0. \tag{3.18}$$

In Smart Grid, if we expect to detect NTL frauds within 6 hours, where the metering interval is set to be 15 minutes typically [36], one observer meter can observe 8 meters at most, and the desired m is 3. In a community with N meters, at least, $\lceil N/8 \rceil$ observer meters should be installed. Inversely, if consider from the angle of saving budget, installing one observer meter for each community is considerable. In the traditional power grid, the time interval for measurement may be much longer than in Smart Grid, because of the difficulty of gathering data. If we can get data once per day, we need at least 24 days to achieve the same effect as in Smart Gird. Now consider saving the detection time and

the budget at the same time. We can set different weights or priorities for the detection time and the budget.

Let's denote w_1 as the weight of the detection time and w_2 as the weight of the number of the observer meters, respectively. Here, fewer observer meters means less budget needed. We define o as the number of the observer meters installed in a community.

Theorem 3.2. *To balance the budget and the detection time in NFD, the number of the observer meters o must satisfy the following equation:*

$$o = \sqrt{\frac{w_1 m N T_0}{w_2}}, \tag{3.19}$$

and the number of meters n monitored by one observer cannot exceed:

$$n \leq \sqrt{\frac{N w_2}{w_1 m T_0}}. \tag{3.20}$$

Proof. Let's define y as:

$$y = w_1 t + w_2 o. \tag{3.21}$$

To balance the budget and the detection time in NFD, y should be minimized. We notice that

$$n = N/o, \tag{3.22}$$

and put n into Eq. (3.18), we get

$$t = mNT_0/o. \tag{3.23}$$

Now, put t into Eq. (3.21), we get

$$\begin{aligned} y &= w_1 t m N T_0/o + w_2 o \\ &\geq 2\sqrt{w_1 m N T_0 w_2}. \end{aligned} \tag{3.24}$$

When $o = \sqrt{\frac{w_1 mNT_0}{w_2}}$, y is the minimal, and the value is $2\sqrt{w_1 mNT_0 w_2}$. Moreover, the related detection time t is $\frac{mNT_0 w_2}{w_1}$.

Correspondingly, according to Eq. (3.22), the number of meters monitored by one observer cannot exceed $\sqrt{\frac{Nw_2}{w_1 mT_0}}$. □

3.5 Conclusion

In this chapter, a novel detector NFD is proposed to detect NTL frauds in Smart Grid. NFD is based on Lagrange polynomials to generate a polynomial for each meter using a small dataset. By comparing the polynomials between the normal meters and the abnormal meters, we can identify tampered meters. Various experiments have been conducted to show the effectiveness of NFD. A detailed discussion about parameter selection, together with mathematical proofs and case study, have guided its way to real-world practical applications. As a future work, we will further study the conjecture in this chapter. Moreover, for the on-line detection algorithm, we will set up a series of experiments to test its false alarm rate and efficiency in real-world applications.

Note that NFD does not like a traditional security solution such as intrusion detection system (IDS) where how to choose a good detection threshold is an important aspect. Instead, NFD uses a non-traditional approach to tackle a security problem. Our focus is not how to choose a better detection threshold, but presenting our method and the foundation of the method in general. How to choose a better threshold will be our future research.

CHAPTER 4

FNFD: FAST NTL FRAUD DETECTION AND VERIFICATION

4.1 Introduction

To improve the detection speed, a detector named FNFD (fast NTL) [28, 29] is proposed in this chapter. FNFD can detect NTL frauds with a small amount of data. The detection speed of FNFD is much faster than the existing detectors. FNFD can detect multiple tamered meters as well as a single tampered meter in a group. Moreover, FNFD has a new function, fraud verification. Fraud verification is to verify a pre-existed NTL fraud. Existing detectors have to redo the whole detection process to verify a fraud, but FNFD only needs one more step. Instead of analyzing user behavior, FNFD analyzes adversary behavior and builds adversary models based on the analysis. The models are built on linear functions, e.g. Recursive Least Square (RLS) [34]. Thus, the detection speed of FNFD is faster than the detector whose model is built on polynomials [26].

4.2 Working Process and Algorithm

We install a central observer meter along the pole side in the community, where a group of n ($n \leq N$) smart meters are connected, shown in Fig. 3.1. The purpose of introducing this observer is to record the total amount of electricity supplied to the n meters. We assume that the measurement of the observer is accurate and it is well-secured. We attach a tamper-resistant device to the observer and monitor it with intensive surveillance. Due to budget and privacy consideration, we cannot equip each meter with a tamper-resistant device and cannot observe each meter closely. The smart meters report power consumption periodically.

Typically, meters are read every 15 minutes in Smart Grid [36]. Therefore, a typical value of T_j is 15 minutes, but T_j could be smaller or larger theoretically. The value of E_{ij} must be greater than the value of x_{ij} if it is an NTL fraud. If it is not an NTL fraud, the value of E_{ij} should be almost the same as x_{ij}. We use a coefficient a_i to represent a meter i, and a_i may have different values in different T_j which is defined as:

$$a_{ij} = E_{ij}/x_{ij}. \tag{4.1}$$

Thus, a meter is normal when $a_{ij} = 1$, and it is tampered when $a_{ij} > 1$. Let's use the notation η as the measurement accuracy. A meter is normal when $1 - \eta \leq a_{ij} \leq 1 + \eta$, and it is tampered when $a_{ij} > 1 + \eta$. Typically, the value of η is set to 2%. We assume that meters have the same measurement accuracy based on the observation that the difference is slight although measurement accuracy varies. To make it concise, we define α_{min} and α_{max} as:

$$\alpha_{min} = 1 - \eta, \tag{4.2}$$

and

$$\alpha_{max} = 1 + \eta, \tag{4.3}$$

respectively. Thus, when $a_{ij} > \alpha_{max}$, the meter is tampered. When $\alpha_{min} \leq a_{ij} \leq \alpha_{max}$, the meter is normal.

a_{ij}, the coefficient of a meter is obtained from the data of one measurement. However, the value a_{ij} varies with T_j for each meter. We should obtain a stable coefficient a_i to represent a meter. If we think of x_{ij} as x and E_{ij} as y, we can get a point B at the coordinate shown in Fig. 4.1. Correspondingly, a group of (x_{ij}, E_{ij}) value pairs have a group of scattered points at the coordinate show in Fig 4.1. We cannot get a function with these points on it. However, finding a line which is the closest to these points is feasible.

We take the coefficient of the line as the coefficient of the meter. The lines are denoted as:

$$f_i(x) = a_i x. \tag{4.4}$$

It is easy to prove that a tampered meter has a line above the line of $f_1(x) = \alpha_{max} x$.

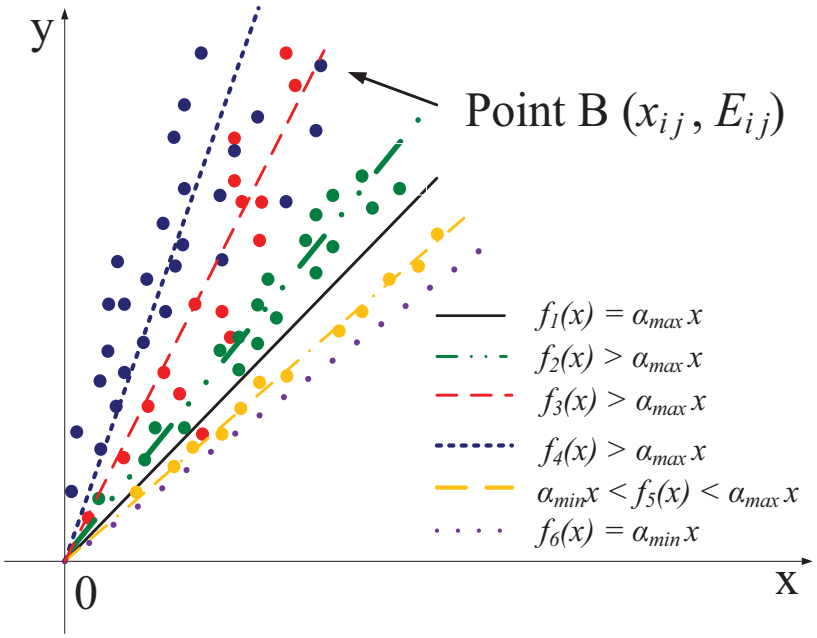

Figure 4.1: Each point at the coordinate represents a pair of values, that is (the amount of the measured electricity, the amount of the consumed electricity) of a meter. A line is used to fit each group of points. The black line is the typical line of a normal meter. A tampered meter has a line above the black line and lines of tampered meters are different.

We only have limited measurement data. How can we generate these lines? We notice that

$$E_j = \sum_{i=1}^{n} E_{ij}, \tag{4.5}$$

and E_j is available since it is recorded by the observer. We re-write it in the following:

$$E_j = \sum_{i=1}^{n} a_i x_{ij}. \tag{4.6}$$

X_j is the vector of the values of the j-th measurement. A is the vector of all

coefficients. We have:

$$A = (a_1, a_2, \ldots, a_n). \tag{4.7}$$

$$X_j = (x_{1j}, x_{2j}, \ldots, x_{nj}). \tag{4.8}$$

We use r_{ij} to denote the distance from a point to the closest line of Meter i in T_j, which is defined as:

$$r_{ij} = E_{ij} - f_i(x_{ij}) \tag{4.9}$$

The closest line is defined as the summation of the distances r_{ij} is the minimal, and the summation is denoted as:

$$S = \sum_{j=1}^{m} r_{ij}^2. \tag{4.10}$$

Now, the problem becomes a Least Square (LS) problem

$$S \to minimum. \tag{4.11}$$

If the data of all the measurements and the values of E_{ij} are available, this problem can be solved via matrix inversion. However, the measurement data are not available and they come in one by one in real time. We do not know E_{ij}, too.

We suppose that an estimation of A is available after $j-1$ times of measurements, which is A_{j-1}. The data of a new measurement X_j and E_j come in, and we need to update A_{j-1} with the new data. Based on the idea of RLS, to get a new estimation A_j, we have:

$$A_j = A_{j-1} + W_j(E_j - X_j A_{j-1}), \tag{4.12}$$

where

$$W_j = P_{j-1} X_j^T (\lambda + X_j P_{j-1} X_j^T)^{-1}, \tag{4.13}$$

$$P_j = (I - W_j X_j) P_{j-1}/\lambda, \tag{4.14}$$

$$P_j^{-1} = \lambda P_{j-1}^{-1} + X_j^T X_j. \tag{4.15}$$

Here, I is the identity matrix. W is an array of weight. The value of P shows the degree of precision of the measurement. P is initialized with $P_0 = kI$, where k is a constant with a high value. λ is a forgetting factor which has a value between 0 and 1 ($0 < \lambda \leq 1$). The main function of λ is to "forget" the old measurements. The level of affection of the old data is decided by the concrete value of λ. The affection decreases with the increase of λ. To decrease the affection of the old data, a smaller value of λ is preferred. Introducing λ to FNFD makes it more flexible in real-world applications, where the situation of each case varies.

Algorithm 2 FNFD: fast NTL fraud detection and verification

1: Initiation: set initial values of n, α_{min}, α_{max}, A_{j-1}, λ and k. Set $P_{j-1} = kI$. j starts from 1 in fraud detection, and starts from any number in fraud verification.
2: **repeat**
3: record the value of observer meter E_j in each time period j,
record the value array of all other meters X_j in each time period j,
$W_j \leftarrow P_{j-1} X_j^T (\lambda + X_j P_{j-1} X_j^T)^{-1}$,
$A_j \leftarrow A_{j-1} + W_j (E_j - X_j A_{j-1})$,
$P_j \leftarrow (I - W_j X_j) P_{j-1}/\lambda$
4: **until** A_j doesn't change
5: **for** each a_i in A_j **do**
6: **if** $a_i > \alpha_{max}$ **then**
7: identified as tampered
8: **if** $\alpha_{min} \leq a_i \leq \alpha_{max}$ **then**
9: identified as normal
10: **else**
11: report error

FNFD fraud detection and verification algorithm is shown in Alg. 2. The processes of detection and verification look similar to each other. In fact, the unified process is one of the attracting features of FNFD which makes things simple. In fraud detection, j has to start from 1 since there are no historical data or estimations available. Moreover, we need to set values for A_0 and P_0 to get started. In fraud verification, j could start from any

number, since A_{j-1} is already known. The verification process may take only one step and we can get a new result.

4.3 Experiments

Various experiments have been carried out to test the performance of FNFD. To show the effectiveness and performance, we conducted the same experiments on FNFD, NFD, DCI, and BCGI, introduced in the related work section earlier. We choose three typical experiments and presented in this section. The parameters are chosen as follows: the value of λ is set to 0.01, k is set to 100, and the value of a_i is 2. The value of η is set to 2%, and correspondingly α_{max} has a value of 1.02, and α_{min} is 0.98. A normal meter has a line falling in the range between 0.98 and 1.02. A tampered meter has a line falling in the range above 1.02. FNFD reports an error when any line of a meter is below 0.98. All the data in the experiments are simulated. Normal consumption range, family/business size, season, weather and other variations are considered when we randomly generate usage data. Then abnormality is added into the normal data.

4.3.1 Detect a Single Tampered Meter

This experiment is to test FNFD on detecting a single tampered meter when the other meters are normal. Table 4.1 shows the data set containing the data of 20 measurements.

The converging process of the coefficients of the 10 meters in Exp. 1 is shown in Fig. 4.2. The coefficients change step by step with the data input of each measurement. After the 10th step, the coefficients of all meters converge to fixed values. The coefficient of Meter 4 converges to 1.33. The other coefficients converge to 1. The converging process shows that Meter 4 is tampered and other meters are normal. The same experiment is conducted to test NFD, and NFD can identify Meter 4 as tampered at the 20th step. The input dataset for NFD contains 20 measurements. It shows that FNFD can double the detection speed of NFD and needs half of the data.

Table 4.1: The unit of the billed electricity usage (kWh) of 10 meters and 1 observer in FNFD - Exp. 1

Meter 1	2	3	4	5	6	7	8	9	10	Observer
2750	3450	5520	2290	3310	9040	4630	3650	5020	5850	46270
2810	3330	6310	3230	1960	9020	5640	2750	5140	6130	47390
2570	4000	6750	3140	2430	9190	5490	2000	5350	6170	48130
2510	3470	6810	2320	3400	10280	6070	5690	7430	7280	56030
3180	3460	5780	2970	5110	9290	6570	3210	5530	5300	51380
2050	4600	7100	3110	6420	9800	6940	3790	5580	6000	56420
3190	3040	7180	3740	2250	8850	6120	3780	5350	5980	50710
2460	3950	5380	1960	3430	9170	5580	4260	2860	6860	46560
3610	4050	5410	2740	3870	9180	5480	3410	6250	6670	51570
2050	3500	4330	3400	3040	9550	5200	4460	6040	5100	47790
2740	3180	5160	2960	5910	8560	5450	3800	5990	5410	50140
2580	30510	5390	2680	6190	7500	6210	3370	5750	4350	48410
2060	3040	5700	3660	4090	7860	6350	2870	3020	3470	43330
2680	4690	5920	2030	5540	9950	7130	3230	4470	4420	50730
2520	3330	6490	3720	5250	9380	7820	3400	4620	6300	54060
3510	3200	6340	4410	4510	9190	7660	2710	4720	6700	54410
3100	3500	5330	4000	4620	8730	5960	2900	5330	6580	51370
2810	4290	5930	4010	5290	9740	6820	3900	5660	6500	56270
2330	4850	6410	2830	3080	10570	6660	4150	5070	6380	53260
2980	3440	6430	2710	4200	9660	6530	4820	6090	6390	54140

The same dataset and experimental settings are used to test BCGI and DCI. However, BCGI cannot work with only one observer (inspector). To observe 10 meters, BCGI needs at least 4 observers which is a huge cost. DCI can identify Meter 4 as the tampered meter at the 7th or 8th step, which is decided by the binary tree structure. In hundreds of experiments that we conducted, this is the best case of DCI. DCI is good at detecting a single tampered meter under the condition that we know there is exactly one tampered meter in a group. However, we cannot get to know how many meters are tampered in advance.

4.3.2 Detect Multiple Tampered Meters

This experiment is to show the effectiveness of detecting multiple tampered meters in a group. Table 4.2 shows the data set containing the data of 20 measurements.

The converging process of the coefficients of the 10 meters in Exp. 2 is shown in

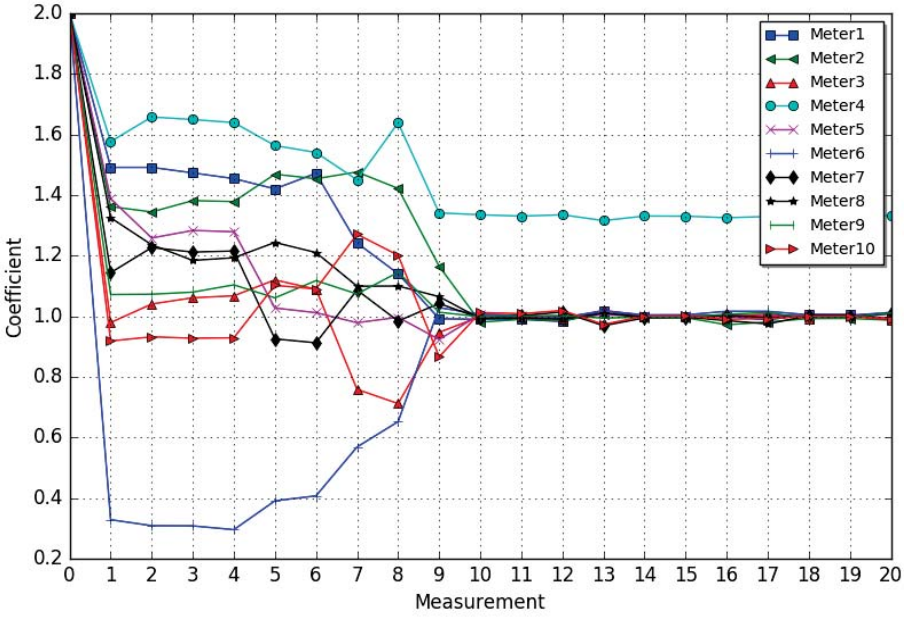

Figure 4.2: The converging process of the coefficients of the 10 meters in Exp. 1. The coefficient of Meter 4 converges to 1.33, while the coefficients of other meters converge to 1. It shows that Meter 4 is the tampered meter.

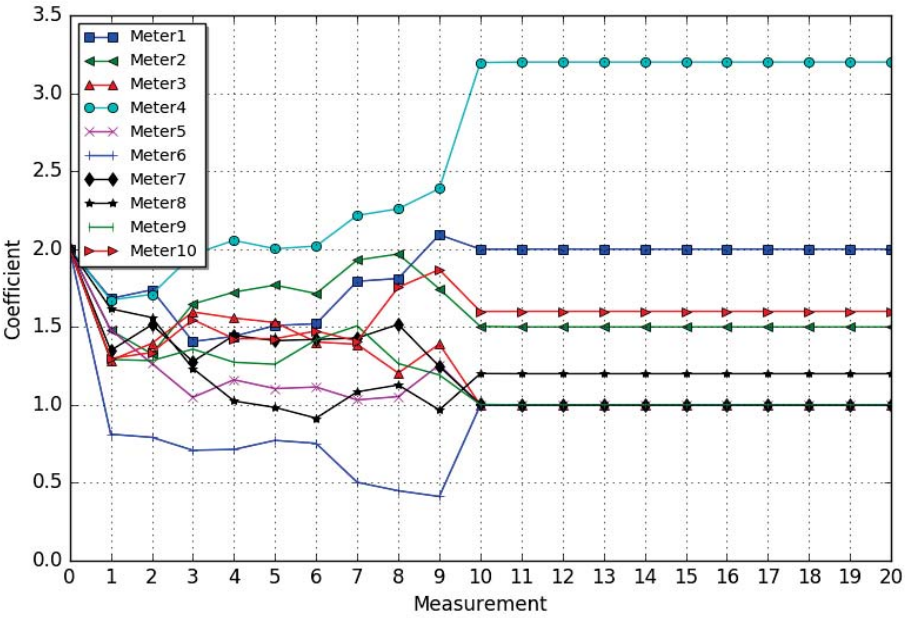

Figure 4.3: The converging process of the coefficients of the 10 meters in Exp. 2. The coefficients of Meters 1, 2, 4, 8 and 10 converge to 2, 1.5, 3.2, 1.2 and 1.6, respectively, and the coefficients other meters converge to 1. It shows that Meters 1,2,4,8 and 10 are tampered and other meters are normal.

Table 4.2: The unit of the billed electricity usage (kWh) of 10 meters and 1 observer in FNFD - Exp. 2

Meter 1	2	3	4	5	6	7	8	9	10	Observer
2190	3620	5520	1950	3160	8620	5390	2990	5530	5590	56802
2220	2980	6310	2700	1890	9300	6030	2650	5330	5600	58550
1890	3510	7110	2720	2330	9060	5120	2570	5780	6790	61097
2330	3640	7060	2060	3270	10690	6050	5070	7470	7060	68632
3090	3160	5610	2750	4650	9130	6300	3800	5280	5630	64258
2480	3860	6110	3440	5820	9290	6950	3920	5830	5290	68926
3360	3550	6660	3610	2450	8000	5930	4390	5610	5560	66411
3130	4010	4810	2510	3380	8270	5830	3790	2190	6400	59575
3080	4360	5460	2660	3480	9120	5670	3540	6330	6520	65952
2440	3980	4230	3490	2390	9440	4880	4140	6610	4980	62504
2180	2510	5820	2160	5540	8230	4650	3450	5730	5140	57371
2850	3390	5120	3040	5450	7650	6430	3680	5860	4310	62335
2780	3280	5540	3220	3970	8530	6260	2970	3050	2790	56162
2480	4610	6380	2470	5430	9400	6570	3330	3630	4640	62609
2280	3500	6710	3920	5420	9990	7310	3110	3710	6470	69578
3400	3170	5810	4160	4680	9110	7270	2740	4360	7070	70697
2560	3810	5060	3830	4520	9120	5610	3330	5290	5820	65999
910	3900	6110	3950	5300	10090	7190	3270	4910	6610	72410
3270	4670	5720	2540	3230	10380	7240	3680	5420	6300	68159
3330	3730	6020	2690	4390	9310	6730	4640	6380	6030	68909

Fig. 4.3. The coefficients change in each step with the data input of each measurement. After the 10th step, the coefficients of the meters converge to fixed but different values. The coefficients of of Meters 1,2,4,8 and 10 converge to 2, 1.5, 3.2, 1.2 and 1.6, respectively. The other coefficients converge to 1. The converging process shows that Meters 1,2,4,8 and 10 are tampered and other meters are normal. The same experiment is conducted to test NFD, and NFD can identify Meters 1,2,4,8 and 10 as tampered at the 20th step. The input dataset for NFD contains 20 measurements. It shows that FNFD can double the detection speed of NFD and needs half of the data.

The same dataset and experimental settings are used to test BCGI and DCI. BCGI cannot normally function and fails to get a result. DCI can identify the tampered meters at the 16th to 19th step, which is up to how the binary tree is constructed. In hundreds of experiments that we conducted, this is the average case of DCI. DCI is not good at

detecting multiple tampered meters in one group.

4.3.3 Detect All Tampered Meters

This experiment is to test the effectiveness of detecting meters in a group that are all tampered. The data set containing the data of 20 measurements is shown in Table 4.3

Table 4.3: The unit of the billed electricity usage (kWh) of 10 meters and 1 observer in FNFD - Exp. 3

Meter 1	2	3	4	5	6	7	8	9	10	Observer
5560	4300	7780	2900	3870	4200	5510	3800	5320	6100	95491.8
6120	3560	5560	3440	2900	5500	6700	3120	6700	7700	98946.8
4230	4500	7780	4900	2670	6100	5340	3000	6200	7400	101094.4
7780	3900	6990	2890	3560	7700	6800	6300	7880	7890	117942.1
7430	4000	6300	3120	5980	8450	7400	4050	5990	5800	112707.4
2670	5300	6440	3800	6880	5560	7340	4560	5670	6120	109290.2
3430	3700	7330	4000	3200	2400	6300	4650	5770	6700	92594.7
8890	3300	5600	2900	3560	6700	5670	4670	3120	2440	86509.9
9700	4400	7120	3650	3780	7120	7400	4100	6670	6870	115164.6
5400	2400	4670	3990	3330	2670	5600	4540	6600	5660	85474.7
6200	3800	5780	3110	6430	4120	6600	4000	6900	5670	102698.2
4560	3900	6340	3440	6280	5230	6670	3890	5900	5220	101089.5
3450	5500	6200	3660	4760	6230	6800	3400	3220	3780	93760.8
5560	4890	6780	3770	5670	6400	7200	3670	4450	4990	104154.9
4670	3700	7400	4120	5980	7400	7900	3670	4560	7450	109674.8
4560	5100	6990	4450	5330	5780	7770	2990	5110	6980	108278.9
3340	4330	7900	4200	4780	2560	6440	3500	5560	6840	97338.7
6320	4990	6550	4320	5550	10530	7780	6700	5880	7330	127063.1
4240	4980	6090	2990	3670	5500	8000	4890	5670	6300	104056.6
5670	3900	5200	3550	5670	9670	8100	4600	6450	9120	119959.7

The converging process of the coefficients of the 10 meters in Exp. 3 is shown in Fig. 4.4. The coefficients change in each step until the 10th step. After the 10th step, the coefficients of the meters converge to fixed but different values. The converging process shows that all the ten meters are tampered meters.

The same dataset and experimental settings are used to test NFD, and NFD can get the same result at the 20th step. The input dataset for NFD contains 20 measurements. It shows that FNFD can double the detection speed of NFD and needs half of the data. The same experiment is conducted to test BCGI and DCI. BCGI still does not function

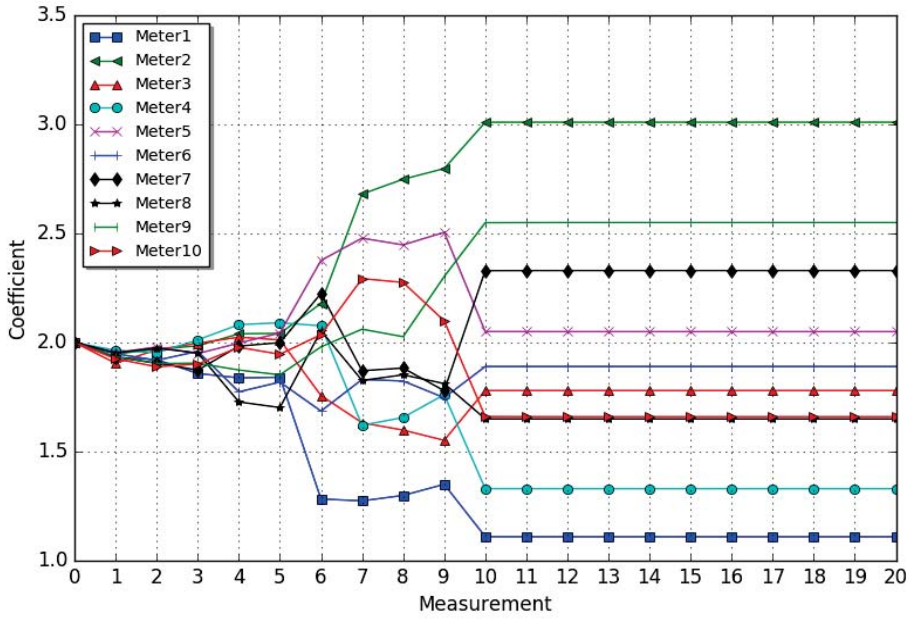

Figure 4.4: The converging process of the coefficients of the 10 meters in Exp. 3. The coefficients of the 10 meters converge to 1.11, 3.01, 1.78, 1.33, 2.05, 1.89, 2.33, 1.65, 2.55 and 1.66, respectively. It shows that all the meters are tampered.

normally. DCI can identify the tampered meters at the 19th step, which is the worst case of DCI. In the worst case, DCI has to inspect each node, including leaves and non-leaf nodes.

4.4 Performance Comparison

We carried out hundreds of experiments to test the performance of FNFD, along with BCGI, DCI and NFD. We will present the experimental results to compare their performance regarding four criteria including fraud detection speed, fraud verification speed, data needed in fraud detection, and data needed in fraud verification. BCGI does not work in all the experiments, and the reason is that BCGI requires much more observers than we can provide. In the worst case, the number of observers that BCGI needs nearly equals to the number of the meters. Even in the best case, the number of observers that BCGI needs is nearly half of the meters. Thus, all the statistics of BCGI are marked as N/A in the figures.

4.4.1 Fraud Detection

We first compare the performance regarding detection speed and data needed in fraud detection. In the experiments, there are no historical data, and thus, FNFD, DCI, NFD, and BCGI start the detection processes from the beginning. To make the results comparable, the speed of NFD is used as the baseline, and we set its speed as 100%. As shown in Fig. 4.5, FNFD is 100% faster than NFD and DCI is 25% faster than NFD. If we compare the speed between FNFD and DCI, FNFD can increase the detection speed of DCI to 160% in average cases.

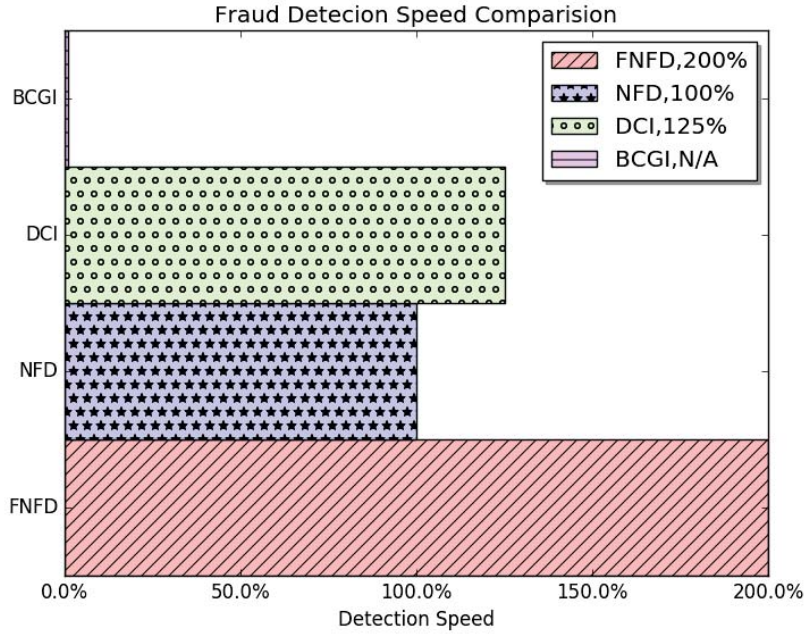

Figure 4.5: Comparing the speed of fraud detection of FNFD, DCI, NFD, and BCGI. The speed of NFD is chosen as the baseline, and its value is set to 100%.

When comparing the data needed in fraud detection, the data needed by FNFD is only half of NFD, shown in Fig. 4.6. When comparing the data needed between FNFD and DCI, FNFD needs 37.5% fewer data than DCI needs in average cases. If we have to compare the performance in the worst cases, the performance of DCI drops rapidly, while FNFD is very stable.

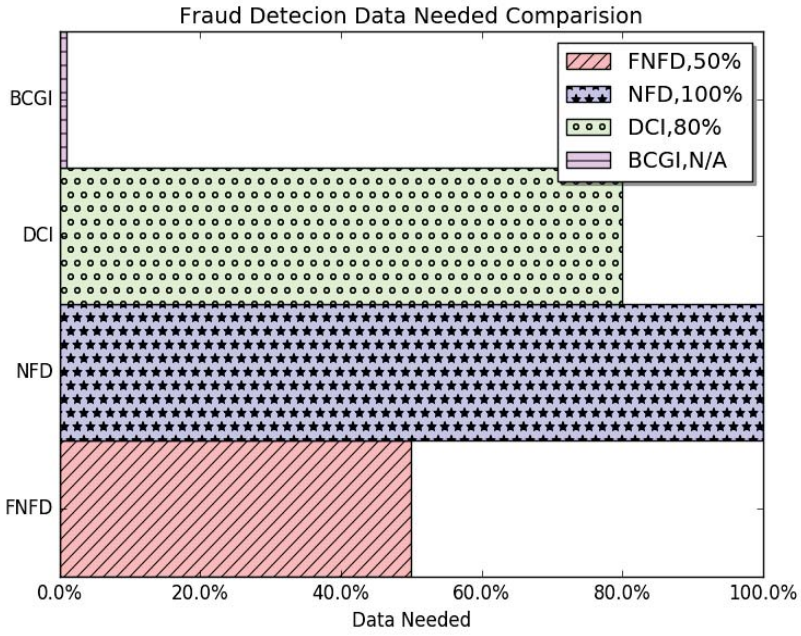

Figure 4.6: Comparing the data needed in fraud detection of FNFD, DCI, NFD, and BCGI. The data needed by NFD is chosen as the baseline, and its value is set to 100%.

4.4.2 Fraud Verification

We first compare the performance regarding verification speed and data needed in fraud verification. In the experiments, FNFD, DCI, NFD, and BCGI all have historical data. As shown in Fig. 4.7, FNFD has a much faster speed than the other three detectors, since FNFD can take the advantage of old data to get a quicker result while the other three have to redo the whole detection processes. As shown in Figs. 4.8, FNFD needs much fewer data than the other three detectors.

Comparing between FNFD and NFD, NFD needs the data from X measurements to verify a fraud, where $X = 2 * \ the\ number\ of\ meters$. In the same case, FNFD only needs the data from one measurement. The performance of DCI is better than NFD but slightly.

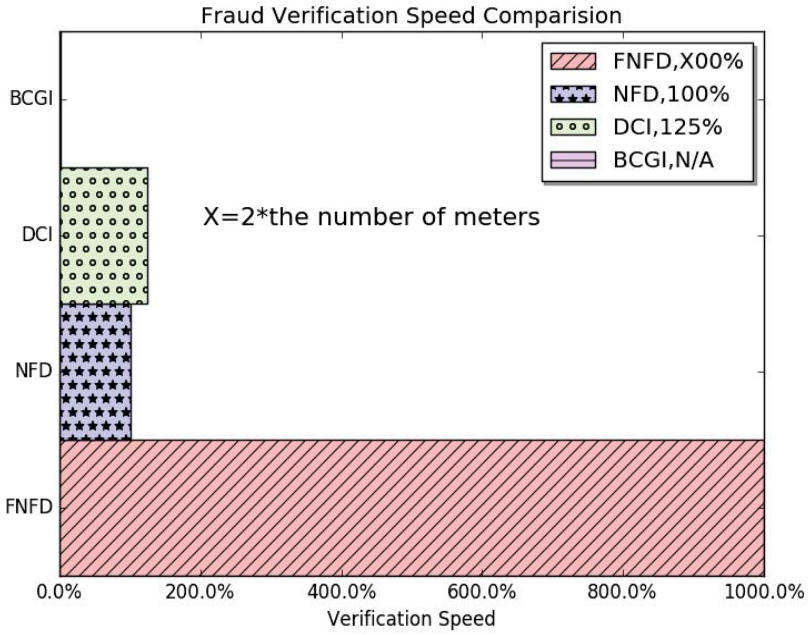

Figure 4.7: Fraud verification speed comparison among FNFD, NFD, BCGI, and DCI. We assume that NFD is the baseline, and set its value to 100%.

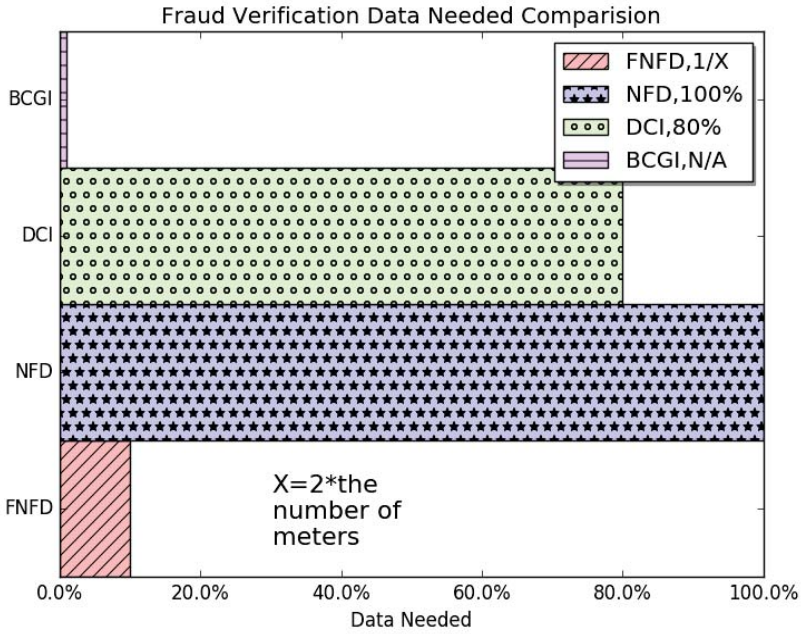

Figure 4.8: Data needed comparison of fraud verification among FNFD, NFD, BCGI, and DCI. We assume that NFD is the baseline, and set its value to 100%.

4.5 Parameter Tuning

In this section, we will study how the parameters affects the detection results and how to choose appropriate parameters. Here we only discuss the relationship between different parameters and fraud detection speed. Fraud verification is not affected by parameter selection, but it strongly relates to the accuracy of historical data. To make the results comparable, we use NFD's detection speed as a baseline. Since the detection speed of NFD is not affected by parameter selection, we assume that the detection speed of NFD is 100%. The values of λ, $A0$ and k do not affect the performance of DCI, but the value of n affects DCI to some extent. Although these parameters do not apply to BCGI, we list it as a reference to show the performance of FNFD.

4.5.1 Tuning k

k is the constant used to initiate P_0. Whether do different values of k affect FNFD's detection speed? Here, we conduct experiments on the same dataset, the same values of all other parameters, but different values of k.

Here, λ is set to be 0.1 and a_{i0} is 2. The number of meters under observation, n, is 10. As shown in Fig. 4.9, the detection speed increases with the increase of the value of k. Thus, to get a faster result of fraud detection, we need a higher value of k. But the speed cannot exceed 200% when k reaches a threshold value, and this threshold value is decided by λ and A_0.

4.5.2 Tuning λ

λ is the forgetting factor, which indicates how the old measurement affects the new result. λ is between 0 and 1. When it is 0, FNFD will not consider the effect of old measures. When the value of λ is 1, FNFD sticks to the old values. Typically, we do not set λ to 0. If we have to set λ to 0, we use a very small value instead, or rewrite Eqs. 4.12, 4.13, 4.14 and 4.15 in other forms to avoid the problem of dividing by zero. We use the same dataset with different values of λ, varying from 0.01 to 1, to test the detection speed

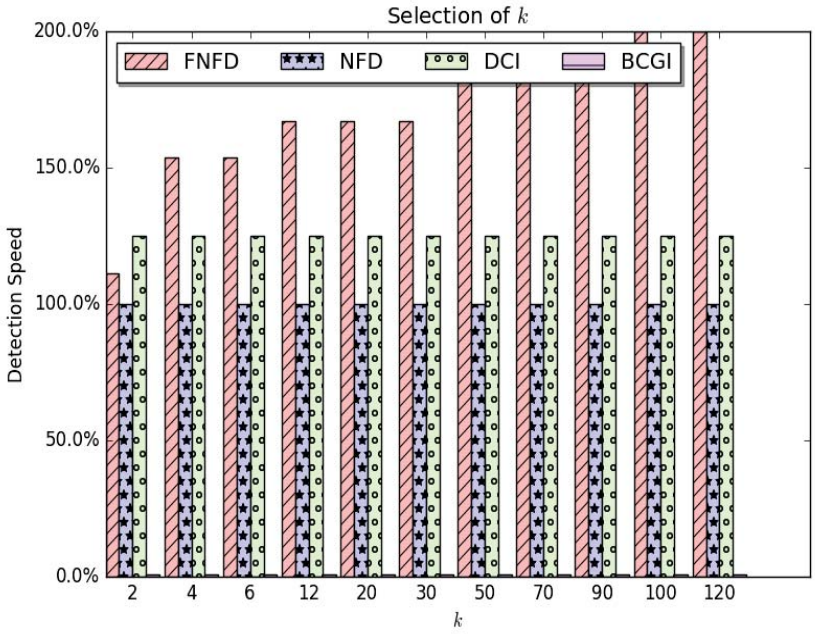

Figure 4.9: Detection speed comparison among FNFD, NFD, BCGI, and DCI with different values of k. Detection speed of FNFD, with all different ks is faster than NFD. When k is bigger, the detection speed is faster. We assume that the detection speed of NFD is 100% and use it as the base line.

of FNFD.

In this experiment, there are 10 meters observed by 1 observer meter. Here, k is set to be 100 and a_{i0} is 6. As shown in Fig. 4.10, the detection speed increases with the decrease of the value of λ. Thus, to get the result faster, we need a smaller λ. But the speed cannot exceed 200% when λ reaches a threshold value, and this threshold value is decided by k and A_0.

4.5.3 Tuning A_0

Another parameter we need to discuss is A_0, the vector of the initial values of the coefficients. Since we have no historical data in fraud detection, we have to choose a good A_0. Since A_0 is the vector of a_{i0}, we show the values of a_{i0} in the experimental results based on the assumption that all a_{i0}s have the same initial value.

Here, k is set to be 100, λ is 0.1 and the number of under-observed meters, n, is 10. Here all values of a_{i0} are larger than 0.98, since a value smaller than 0.98 indicates an error

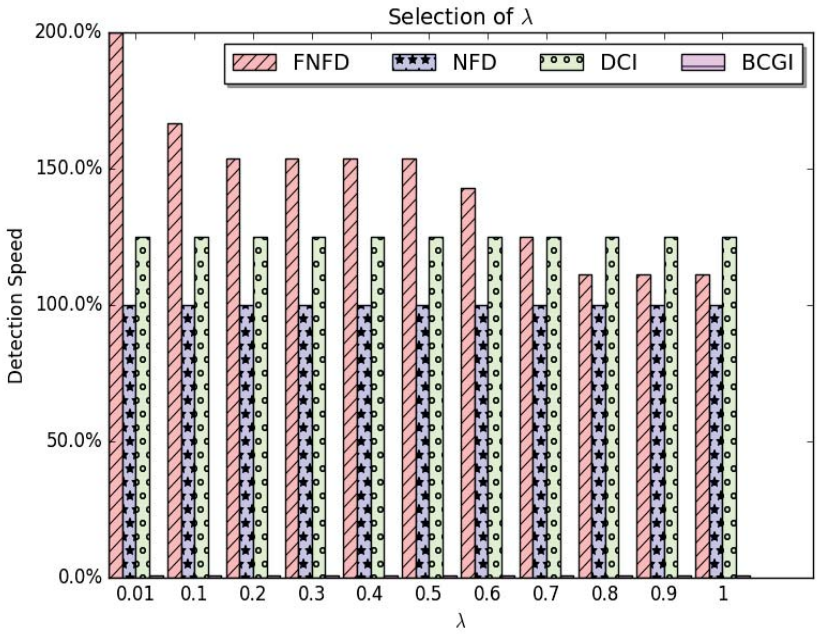

Figure 4.10: Detection speed comparison among FNFD, NFD, BCGI, and DCI with different values of λ. When λ is smaller, the detection speed is faster. We assume that the detection speed of NFD is 100% and use it as the base line.

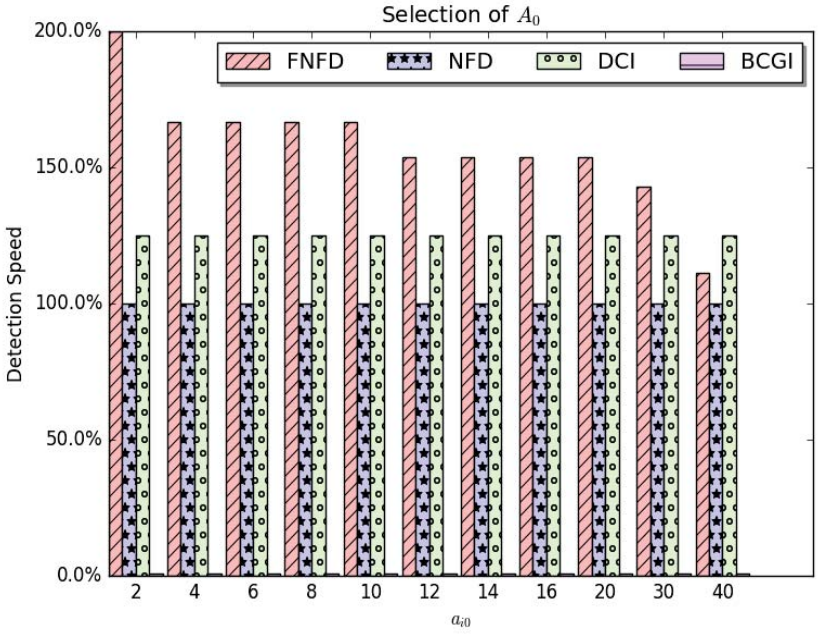

Figure 4.11: Detection speed comparison among FNFD, NFD, BCGI, and DCI with different values of a_{i0}. When a_{i0} is smaller, the detection speed is faster. We assume that the detection speed of NFD is 100% and use it as the baseline.

occurs. As shown in Fig. 4.11, the detection speed increases with the decrease of the initial value of A. Therefore, a larger A_0 will improve FNFD's detection speed. But the speed cannot exceed 200% when A_0 reaches a threshold value, and this threshold value is decided by k and λ.

4.5.4 Tuning n

n is the number of meters observed by one observer meter. For a group of meters, we could install multiple observer meters to monitor the group, and extremely, we could install an observer for each meter, and we can easily figure out the tampered meters. However, it is not possible because of budget constrain. Moreover, this is also the reason why BCGI is not applicable. We can also install only one observer for a large group to save budget, but it is time-consuming to get a result from such a large dataset.

Theorem 4.1. *To achieve the best effect on both the detection time and the budget, the number of the observer meters o must satisfy the following equation:*

$$o = \sqrt{\frac{w_1 N T_0}{w_2}}, \tag{4.16}$$

and the number of users n under one observer cannot exceed:

$$n \leq \sqrt{\frac{N w_2}{w_1 T_0}}. \tag{4.17}$$

Here,

- w_1 is the weight of the detection time;
- w_2 is the weight of the number of the observer meters (less observer meters means less budget needed);
- o is the number of the observer meters installed in a community.

Proof. Let's define

$$y = w_1 t + w_2 o. \tag{4.18}$$

To get the best effect on both the detection time and the budget, y should obtain its minimum value. Let's define the desired detection time as t, and t is calculated as:

$$t = nT_0. \tag{4.19}$$

Since

$$n = N/o, \tag{4.20}$$

put it into Equ. (4.19), and we get

$$t = NT_0/o. \tag{4.21}$$

Now, put Equ. (4.21) into Equ. (4.18), and we get

$$\begin{aligned} y &= w_1 t N T_0/o + w_2 o \\ &\geq 2\sqrt{w_1 N T_0 w_2}. \end{aligned} \tag{4.22}$$

When $o = \sqrt{\frac{w_1 N T_0}{w_2}}$, y obtains its minimum value $2\sqrt{w_1 N T_0 w_2}$. Moreover, the related detection time t is $\frac{N T_0 w_2}{w_1}$.

Correspondingly, according to Eq. (4.20), the number of users under one observer cannot exceed $\sqrt{\frac{N w_2}{w_1 T_0}}$. □

This theorem shows how the absolute detection speed is affected by n. Both the detection speed of NFD and FNFD increase with the decrease of n. But n cannot exceed $\sqrt{\frac{N w_2}{w_1 T_0}}$, to get the best balanced effect.

To show how the relative detection speed affected by n, we conduct several experiments on different sizes of dataset, n. k is set to 100, a_{i0} is 6, and λ is 0. As shown in Fig. 4.12, the relative detection speed of FNFD is not affected by n. The detection speed of

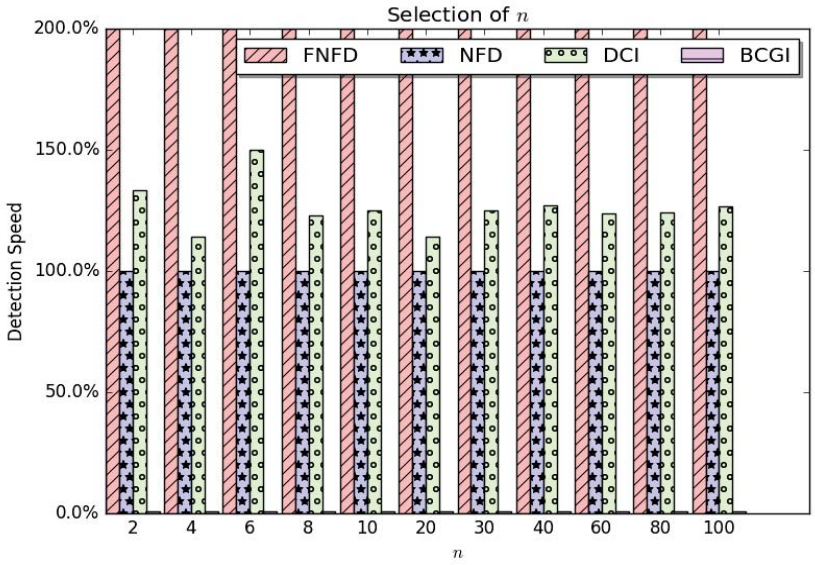

Figure 4.12: Detection speed comparison among FNFD, NFD, BCGI, and DCI with different values of n. n affects absolute detection speed of both NFD and FNFD, but doesn't affect their relative speed comparison. We assume that the detection speed of NFD is 100% and use it as the baseline.

DCI is affected by n. It is because when the number of meters changes, the tree structure also changes with it. We did a dozen of experiments to test the detection speed of DCI with different values of n, and the detection speed considering average cases are listed. This serials of experiments also show the accuracy of FNFD when it scales with the number of meters.

4.6 FNFD Stability and Convergence

In this section, we will study the stability and convergence of FNFD algorithm.

4.6.1 FNFD Stability

Stability means that we can still find an approximate solution when the accuracy class or error of the computation changes. Here, stability refers to the stability of the algorithm. The performance of FNFD is stable, as we discussed in the experiments. But, as an algorithm, FNFD is not stable, because when we change the accuracy class, some of

the A_j will jump into another basket when comparing to α_{min} and α_{max}. But we can increase its stability by imposing bounds on its relative precision, and we will study it in our future work.

4.6.2 FNFD Convergence

Convergence means the algorithm can always get a solution. As shown in Alg. 2, FNFD can get a solution when A_j doesn't change. Here, we will prove that FNFD is convergent if and only if its input data set, X_j is persistent exciting, where $0 < \lambda < 1$. Moreover, when $\lambda = 1$ FNFD is not convergent.

Here, the input data set is persistent exciting if it changes sufficiently to "excite" the system so that the dynamics of the system can be captured, and it is formally defined as follows:

Definition 4.1. *The input data set X_j is persistent exciting, if for some constant s and all l, there exist positive constants β and θ such that*

$$\beta I \leq \sum_{i=l}^{l+s} X_i^T X_i \leq \theta I. \tag{4.23}$$

To prove FNFD is convergent and to obtain its constraint, we need to prove the following three lemmas first.

Lemma 4.1. *If the input data set X_j is persistent exciting and $0 < \lambda < 1$, for all $j \geq s$, the following inequation holds*

$$P_{j-1}^{-1} \geq \frac{\beta(1-\lambda)\lambda^s}{1-\lambda^{s+1}} I. \tag{4.24}$$

Proof. From Eq. 4.15 and Eq. 4.23, we get

$$\begin{aligned}(P_{l-1}^{-1} + P_l^{-1} + \cdots + P_{l+s-1}^{-1}) &= \lambda P_{l-2}^{-1} + X_{l-1}^T X_{l-1} + \cdots \\ &\quad + \lambda P_{l+s-2}^{-1} + X_{l+s-1}^T X_{l+s-1} \\ &\geq \sum_{j=l}^{l+s} X_{j-1}^T X_{j-1} \\ &\geq \beta I.\end{aligned} \tag{4.25}$$

From Eq. 4.15, we get

$$\frac{1}{\lambda} P_{j-1}^{-1} \geq P_{j-2}^{-1}, \tag{4.26}$$

so that for all l, $1 \leq l \leq n$

$$(\frac{1}{\lambda^s} + \frac{1}{\lambda^{s-1}} + \cdots + 1) P_{l+s-1}^{-1} \geq \beta I. \tag{4.27}$$

Therefore, for all $j \geq s$

$$P_{j-1}^{-1} \geq \frac{\beta(1-\lambda)\lambda^s}{1-\lambda^{s+1}} I. \tag{4.28}$$

□

Lemma 4.2. *FNFD is convergent if its input data set X_j is persistent exciting and $0 < \lambda < 1$.*

Proof. Let

$$V_j = A_j^T P_{j-1}^{-1} A_j. \tag{4.29}$$

Based on Eqs. 4.12, 4.13 and 4.15, we have

$$\begin{aligned} V_j - V_{j-1} &= A_j^T P_{j-1}^{-1} A_j - A_{j-1}^T P_{j-2}^{-1} A_{j-1} \\ &= A_{j-1}^T [(\lambda - 1) P_{j-2}^{-1} - \frac{\lambda X_{j-1}^T X_{j-1}}{\lambda + X_{j-1} P_{j-2} X_{j-1}^T}] A_{j-1} \\ &\leq (\lambda - 1) A_{j-1}^T P_{j-2}^{-1} A_{j-1} \\ &= (\lambda - 1) V_{j-1}. \end{aligned} \tag{4.30}$$

Thus,

$$V_j \leq \lambda V_{j-1} \leq \lambda^j V_0 = \lambda^j A_0^T P_{-1}^{-1} A_0 = k \lambda^j A_0^T A_0 \tag{4.31}$$

Since X_j is persistent exciting, Eq. 4.24 holds based on Lem. 4.1. From Eqs. 4.15, 4.24 and 4.29, we can conclude that for all $j \geq s$

$$\|A_j\|^2 \leq \frac{k(1 - \lambda^{s+1})}{(1 - \lambda)\lambda^s} \lambda^j \|A_0\|^2 . \tag{4.32}$$

Therefore, FNFD is convergent. □

Lemma 4.3. *The input data set X_j is persistent exciting if FNFD is convergent.*

Proof. According to the definition of P in RLS,

$$P_j = E(\epsilon_j \epsilon_j^T), \tag{4.33}$$

where $\epsilon_j = A - A_j$. A_j is convergent, which implies that P_j and P_j^{-1} are bounded. Suppose that for all j

$$b \leq \left\| P_j^{-1} \right\| \leq c, \tag{4.34}$$

where b, c are two positive constants. From Eq. 4.15, we get

$$\begin{aligned} P_{j-1}^{-1} &= \lambda P_{j-2}^{-1} + X_{j-1}^T X_{j-1} \\ &= \lambda^s P_{j-s-1}^{-1} + \sum_{i=0}^{s-1} \lambda^i X_{j-i-1}^T X_{j-i-1} \\ &\geq bI. \end{aligned} \tag{4.35}$$

Choose s so that

$$\lambda^s c \leq \frac{b}{2}. \tag{4.36}$$

Then we get

$$\frac{b}{2} I \leq \sum_{i=0}^{s-1} \lambda^i X_{j-i-1}^T X_{j-i-1} \leq cI. \tag{4.37}$$

Therefore, X_j is persistent exciting. □

Theorem 4.2. *FNFD is convergent if and only if its input data set, X_j is persistent exciting and $0 < \lambda < 1$.*

Proof. Based on Lemma 4.2 and Lemma 4.3, Theorem 4.2 is established. □

4.7 Conclusion

A fast detector, named FNFD, was proposed to detect NTL frauds in Smart Grid. The basic idea is to model adversary's behavior mathematically using RLS. We conducted various experiments to show the effectiveness and outstanding performance of FNFD. Experimental results show that FNFD is 100% faster than NFD and 60 % faster than DCI regarding detection speed. Regarding data needed in fraud detection, FNFD needs 50% fewer data than NFD and 37.5% fewer data than DCI. BCGI failed to get results in all the experiments. We studied parameter tuning in FNFD theoretically and experimentally. We further studied the stability and convergence of FNFD theoretically. As a study result, the algorithm of FNFD is not stable but convergent. In the future, we will improve the stability of FNFD and validate its performance in the real applications in the utility.

CHAPTER 5

CNFD: COLLUDED NTL FRAUD DETECTION

5.1 Introduction

The traditional NTL fraud detection methods attempt to identify a tampered meter or multiple tampered meters among meters [21, 32, 61]. However, an NTL fraud can be very sophisticated. In our recent studies, we discovered a new potential type of frauds, a variant of NTL frauds, called Colluded Non-Technical Loss (CNTL) frauds in the Smart Grid. In a CNTL fraud, more than one fraudster can co-exist or collaborate to commit the fraud. In other words, in a single tampered meter, there are multiple fraudsters. They may not realize the existence of other fraudsters, and we call them co-existing fraudsters. On the other hand, they may realize the existence of other fraudsters and collaborate to commit an NTL fraud, and then we call them collaborating fraudsters. We study the behaviors of the co-existing and collaborating fraudsters and analyze the features of CNTL frauds. We classify CNTL frauds into four types: segmented CNTL frauds, fully overlapped CNTL frauds, partially overlapped CNTL frauds, and combined CNTL frauds.

In this chapter, a novel detector, called Colluded Non-Technical Loss Fraud Detection (CNFD), is proposed to address the CNTL fraud problem in Smart Grid. CNFD has two steps to detect CNTL frauds: 1) NTL fraud detection and 2) fraudster differentiation. In the NTL fraud detection step, CNFD quickly identifies the tampered meter within a group of meters. In the fraudster differentiation step, CNFD differentiates multiple fraudsters in the tampered meter. CNFD adapts Recursive Least Square (RLS) [34] to model fraudsters' behaviors using linear functions. Different fraudsters have different models to represent themselves. CNFD is lightweight and requires only a small

amount of data. CNFD can even predict the behaviors of fraudsters which they may not realize by themselves. We have conducted various experiments to test the effectiveness and performance of CNFD. The experimental results show that CNFD can effectively detect four types of CNTL frauds and describe the behaviors of different fraudsters clearly.

5.2 Colluded NTL Fraud

A CNTL fraud occurs when multiple fraudsters tamper with a meter so that the meter records less electricity than the consumed amount by the household, and the fraudsters gain illegal benefit by paying less money. After further analyzing these fraudsters, we find that they have different behaviors which they may not realize themselves. Moreover, the behaviors of how they collude the frauds can be different.

Sometimes, when a meter is tampered with by multiple fraudsters, these fraudsters may commit the malicious manipulation at different time segments. As shown in Fig. 5.1(a), we name this kind of CNTL frauds as segmented CNTL frauds. In a segmented CNTL fraud, fraudsters usually do not realize the existence of other fraudsters. Thus, these fraudsters are co-existing fraudsters, and are not collaborating fraudsters.

During most of the time, CNTL frauds are not segmented. Different fraudsters can manipulate the same meter at the same time, or at least part of the manipulation time overlaps. We call this kind of colluded NTL frauds as overlapped CNTL frauds. Overlapped CNTL frauds can be classified into partially overlapped CNTL frauds and fully overlapped CNTL frauds, as shown in Figs. 5.1(b) and (c), respectively. The difference between partially overlapped CNTL and fully overlapped CNTL is that there is one fraudster who overlaps all other fraudsters in a fully overlapped CNTL fraud. This feature can easily fool a detector and can make the detector believe that there is only one fraudster in this meter.

Some frauds are even more complicated since they have both segmented CNTL and overlapped CNTL, and we name them as combined CNTL frauds, shown in Fig. 5.1(d). In

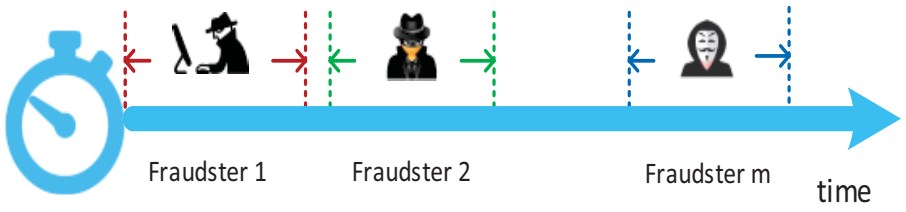

(a) Segmented CNTL fraud

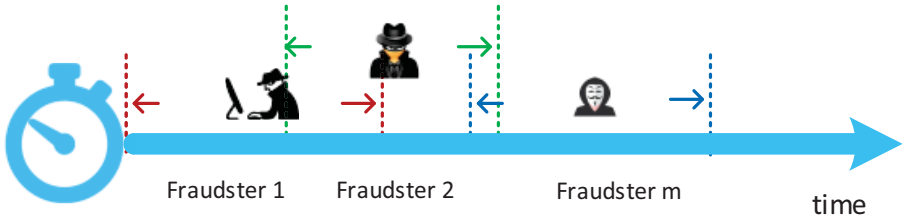

(b) Partially overlapped CNTL fraud

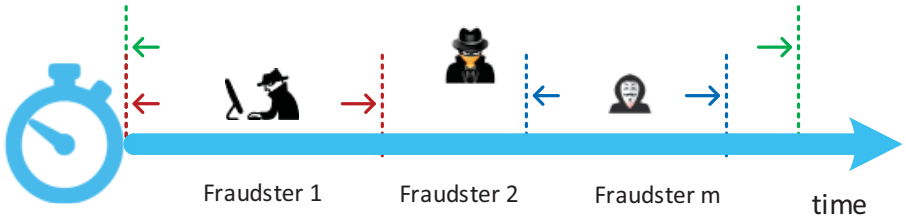

(c) Fully overlapped CNTL fraud

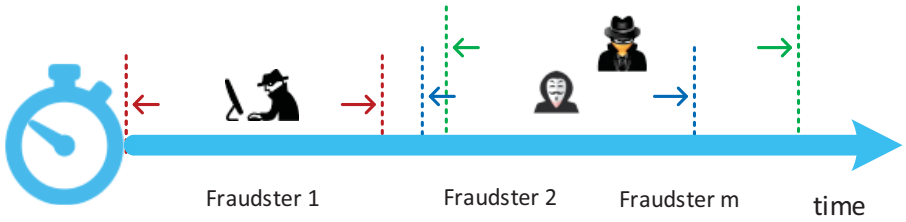

(d) Combined CNTL fraud

Figure 5.1: Four different types of CNTL frauds that we discovered. a) Segmented CNTL fraud; b) Partially overlapped CNTL fraud; c) Fully overlapped CNTL fraud; d) Combined CNTL fraud.

an overlapped CNTL fraud or a combined CNTL fraud, fraudsters may or may not realize the existence of other fraudsters. Thus, these fraudsters could be co-existing fraudsters, or they could also be collaborating fraudsters.

5.3 CNTL Fraud Detection

In this section, we will introduce how to detect CNTL frauds using our proposed CNFD method, and the algorithm of CNFD is also presented.

5.3.1 Observer Meter

We install an observer meter to record the total amount of electricity supplied to $n(n \leq N)$ households in this community. The observer meter is installed at the pole side keeping a distance to the properties of these households. Among these n households, one or multiple meters are suspected to be tampered with. To guarantee the safety of the observer, we attach a tamper-resistant device to the observer and monitor it intensively using a camera. The tamper-resistant device is to protect the observer from cyber attacks. Camera surveillance is to protect the observer from any physical tampering. The observer meter is shown in Fig. 3.1. There are two reasons that we cannot secure all the meters using the way that we secure the observer. One reason is the limited budget. Another reason is privacy consideration [25, 27, 30, 38, 39].

The smart meters owned by the households are responsible for keeping records of the energy consumptions of the households. The metering system will automatically read these meters, including smart meters and the observer. The interval of meter reading is fixed, but the length of the interval is adjustable, e.g. from several minutes to several months. A typical interval is 15 minutes [16, 36]. Now, we have two set of known values. One set is the energy consumption reported by smart meters. Note that the reported value may be smaller than the amount of the actual energy consumption of the household due to the fraud. Another value is the total amount supplied to the $n(n \leq N)$ households. Our objective is to figure out which meters have CNTL frauds.

5.3.2 Tampered Meter Detection

CNFD includes two steps. The first step is to detect tampered meters.

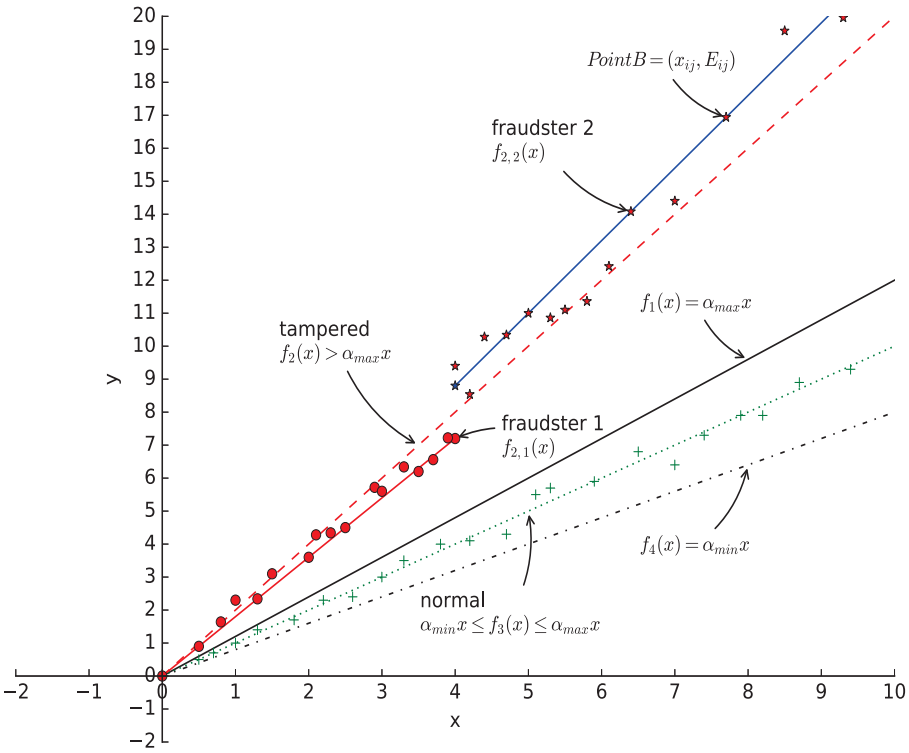

Figure 5.2: Modeling the behavior of fraudsters mathematically and differentiating them. Each value pair, e.g. *(the recorded amount of electricity , the actually consumed amount of electricity)* has a point to represent it at the coordinate. Each meter has a dataset containing a series of value pairs obtained from several measurements. The dataset has a set of corresponding points. In CNFD, a line which represents the set of points is used to represent the meter. For tampered meters, their lines are above the line of $f_1(x) = \alpha_{max}x$. For normal meters, their lines are between the lines of $f_1(x) = \alpha_{max}x$ and $f_4(x) = \alpha_{min}x$. Some lines can be reshaped into multiple lines.

The values of $(E_{ij}, j = 1, 2, \cdots, m)$ are not available although the values of $(x_{ij}, j = 1, 2, \cdots, m)$ are available. For a value pair (x_{ij}, E_{ij}), there is a corresponding point, such as Point B, at the coordinate as shown in Fig. 5.2. Each meter has a group of points of its own, and we can find a line closet to these points to represent this meter. Let

us denote this line as:

$$f_i(x) = a_i x. \tag{5.1}$$

Note that each line starts from $(0, 0)$, since the recorded value must be 0 if the consumed energy is 0.

If Meter i is a normal meter, either $E_{ij}/x_{ij} = 1$ holds or $|E_{ij}/x_{ij} - 1|$ is very small. If $|E_{ij}/x_{ij} - 1|$ is large, this indicates that Meter i is an abnormal (tampered) meter. Define $\alpha_{ij} = E_{ij}/x_{ij}$ which indicates the accuracy ratio, i.e., the error committed by Meter i during the period j. For simplicity and without losing generality, we assume that if Meter i is a normal meter, its α_{ij} should be in the range as follows:

$$\alpha_{ij} \in [\alpha_{min}, \alpha_{max}], (1 \leq i \leq n).$$

The accuracy of metering is affected by many factors, including connection type, power factor, current, standards in different countries, etc. A typical metering system accuracy is $\pm 1.55\%$ [53]. To accommodate rounding error and data noise, we choose $\pm 2\%$ as the accuracy class, i.e., $\alpha_{min} = 0.98$ and $\alpha_{max} = 1.02$. We also assume that if one meter is tampered with (abnormal), we have $\alpha_{ij} > \alpha_{max}$. In other words, we assume that all of the normal meters have the same accuracy range as the above, and all of the abnormal (tampered) meters have higher accuracy values above the range. Generally speaking, α_{ij} could be less than α_{min}, and this means that the billing amount of electricity is larger than the consumed amount so that the customer has to pay more money. The customer herself (himself) will never tamper with a meter in this way. It only happens when a meter is manipulated by outside attackers and the meter readings are altered to be higher than the actual values. However, it is not an NTL fraud in this situation, and it is out of the scope.

As shown in Fig. 5.2, a tampered meter has a line above the line of $f_1(x) = \alpha_{max} x$, and a normal meter has a line between the lines of $f_1(x) = \alpha_{max} x$ and $f_4(x) = \alpha_{min} x$. A line below the line of $f_4(x)$ is a sign of working error. We can figure out which meters are

tampered with and obtain the coefficient vector A. We notice that

$$E_j = \sum_{i=1}^{n} E_{ij}, \tag{5.2}$$

and E_j is available. We re-write it as follows:

$$E_j = \sum_{i=1}^{n} a_i x_{ij}. \tag{5.3}$$

Let X_j be the values of the j-th measurement. Let A be the array of all coefficients. We have:

$$A = (a_1, a_2, \ldots, a_n). \tag{5.4}$$

$$X_j = (x_{1j}, x_{2j}, \ldots, x_{nj}). \tag{5.5}$$

Suppose that we have an estimation of A after $j-1$ times of measurements, A_{j-1}. Now we obtain a new measurement X_j and E_j, and want to update the estimation with this new measurement. According to the theory of Recursive Least Square (RLS), to get a new estimation A_j, we have:

$$A_j = A_{j-1} + W_j(E_j - X_j A_{j-1}), \tag{5.6}$$

where

$$W_j = P_{j-1} X_j^T (\lambda + X_j P_{j-1} X_j^T)^{-1}, \tag{5.7}$$

$$P_j = (I - W_j X_j) P_{j-1}/\lambda, \tag{5.8}$$

$$P_j^{-1} = \lambda P_{j-1}^{-1} + X_j^T X_j. \tag{5.9}$$

Here, W is a weight array. I is the identity matrix. P is the degree of precision of the measurement, and is initialized with $P_0 = kI$, where k is a high value constant. λ is a

forgetting factor with a value between 0 and 1 ($0 < \lambda \leq 1$). In order to reduce the influence of old values, we should choose a lower value of λ.

Let us set j as 1, since we have no historical data, and thus have no knowledge of A. As shown in Alg. 3, the process is repeated until the value of A does not change. Then, each a_i in A is compared to α_{min} and α_{max}. If a_i is larger than α_{max}, Meter i is identified as 'tampered'. Then the value of i is assigned to t.

5.3.3 Fraudster Differentiation

The second step of CNFD is fraudster differentiation. We identified the tampered meter, Meter t, in the first step, and the value of the coefficient vector A is known. In this step, CNFD will try to find out whether there are multiple fraudsters in the tampered meter and differentiate them. An illustrative example is shown in Fig. 5.2. In the first step, the red points are used to generate a red line, $f_2(x)$, which is above the line of $f_1(x) = \alpha_{max}x$. Thus, the meter represented by the red points is identified as the tampered meter. After further analysis, we find that the red points can be reshaped into two lines which are $f_{2,1}(x)$ and $f_{2,2}(x)$. The red dot points are closer to $f_{2,1}(x)$ rather than $f_2(x)$, and the red star points are closer to $f_{2,2}(x)$ rather than $f_2(x)$. In fact, there are two fraudsters and their behaviors are represented by $f_{2,1}(x)$ and $f_{2,2}(x)$, respectively.

The algorithm of CNFD is shown in Alg. 3, which includes the two steps. The codes from Line 15 to Line 20 in Alg. 3 show the process of fraudster differentiation. The basic idea of fraudster differentiation is to calculate the coefficients at every interval after isolating the tampered meter, and analyze the similarity of these values within a given error e. Finally, these values are identified as belonging to different fraudsters. Here, e is a given value of error that defined by users. S_t contains the output coefficients of all the fraudsters in Meter t. S_t is set initially to be an empty set. If the output coefficients in S_t are very similar, within the range of e, it means that there is only one fraudster. In other words, it is not a CNTL fraud.

Algorithm 3 CNFD: CNTL fraud detection

1: Initiation: set initial values of e, n, m, α_{min}, α_{max}, A_{j-1}, λ and k. Set $P_{j-1} = kI$. j starts from 1. Set $S_t = \{\}$, $t = -1$.
2: **repeat**
3: record the value of observer meter E_j in each time period j,
record the value array of all other meters X_j in each time period j,
$W_j \leftarrow P_{j-1}X_j^T(\lambda + X_jP_{j-1}X_j^T)^{-1}$,
$A_j \leftarrow A_{j-1} + W_j(E_j - X_jA_{j-1})$,
$P_j \leftarrow (I - W_jX_j)P_{j-1}/\lambda$
4: **until** A_j doesn't change
5: **for** each a_i in A_j **do**
6: **if** $a_i > \alpha_{max}$ **then**
7: identified as 'tampered'
8: $t \leftarrow i$
9: **if** $\alpha_{min} \leq a_i \leq \alpha_{max}$ **then**
10: identified as 'normal'
11: **else**
12: report 'error' and exit
13: **if** $t = -1$ **then**
14: report 'normal' and exit
15: **for** each $j \leq m$ **do**
16: $a_{tj} = \dfrac{E_j - \sum_{i=1}^{n} a_i x_{ij}}{x_{tj}} (i \neq t)$
17: **for** each a_k in S_t **do**
18: **if** $a_{tj} \geq a_k + e$ **or** $a_{tj} \leq a_k - e$ **then**
19: $S_t = S_t \cup \{a_{tj}\}$
20: Output: S_t.

5.4 Experiments

In this section, we will introduce four experiments to show the effectiveness of CNFD. These four experiments show results of detecting segmented CNTL frauds, fully overlapped CNTL frauds, partially overlapped CNTL frauds, and combined CNTL frauds, respectively. The user defined error e is set to 0.5%. There are 30 measurement records in each experiment, but we only list the first 20 records to save space. The value of k is 100, λ is 0.01, and a_i is 2. We set the measurement accuracy class as 2%, i.e., $\alpha_{min} = 0.98$ and $\alpha_{max} = 1.02$. If a meter's line falls in the range between $y = 0.98x$ and $y = 1.02x$, it is a normal meter. Any line of a meter that is above $y = 1.02x$ is a tampered meter's line. It indicates that an error occurs if there is any line of a meter is below $y = 0.98x$. The data used in the experiments are synthetic data. We obtained normal electricity consumption data based on a real-world dataset [19], and increased the consumption of some meters randomly. The measurement interval is one month.

5.4.1 Experiment 1: Segmented CNTL

In the first experiment, there are 10 meters under the observation of one observer meter. The recorded values and the total supplied value of electricity are listed in Table 5.1.

As shown in Fig. 5.3, this is the tampered meter detection process in Exp. 1, which shows that Meter 4 is a tampered meter and the line of $y = 2.216x$ represents its fraudster's behavior. After further analysis, we find that there are two fraudsters in this meter. Their behaviors are represented by $y = 1.22x$ and $y = 2.22x$, which are shown in Fig. 5.4. Each of the two fraudsters dominates a time segment of the whole process, and therefore it is a segmented CNTL fraud.

5.4.2 Experiment 2: Fully Overlapped CNTL

In the second experiment, there is one observer meter, and it monitors 10 other meters. We list the first 20 measurement records in Table 5.2.

As shown in Fig. 5.5, this is the detection process in Exp. 2. The coefficient of

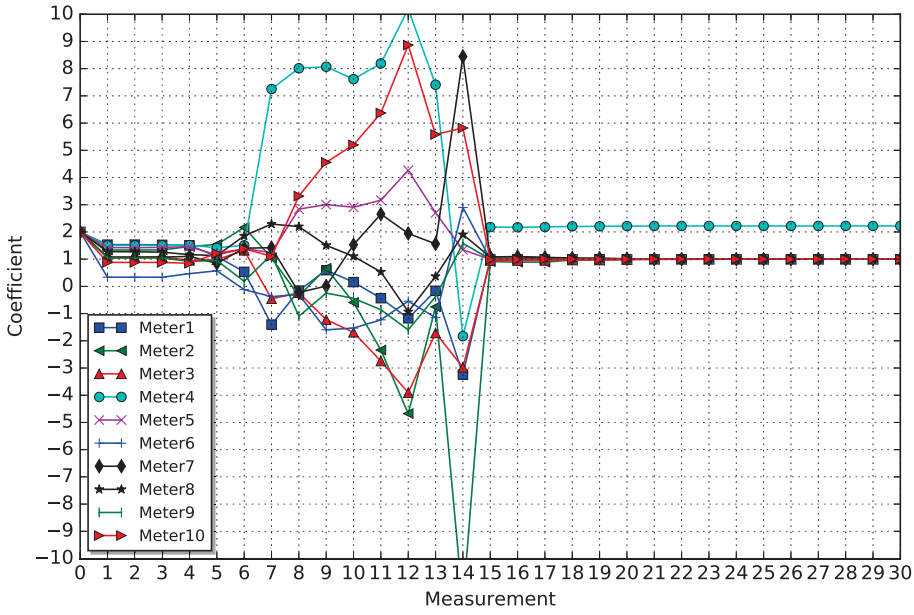

Figure 5.3: The tampered meter detection process in Exp. 1: the converging process of the coefficients of 10 meters. Among these 10 meters, the coefficient of Meter 4 converges to 2.216 while others converge to 1, and this indicates that Meter 4 is a tampered meter.

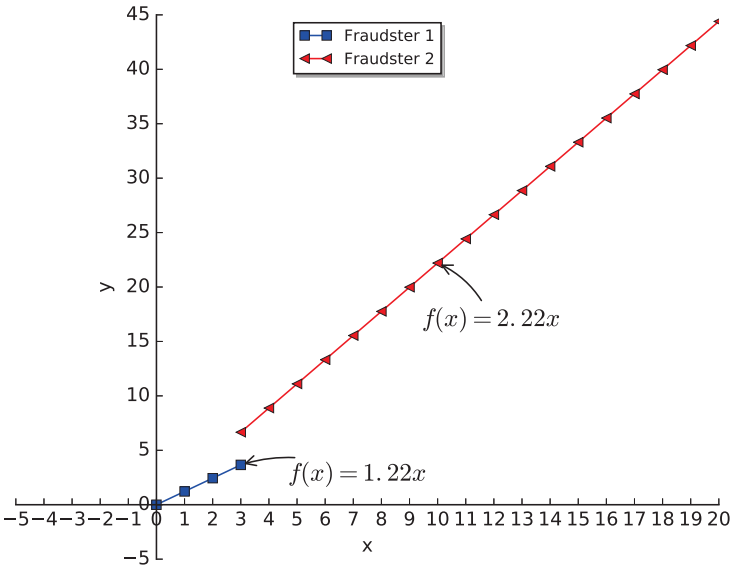

Figure 5.4: The final detection result of CNFD in Exp. 1. CNFD detection shows that there are two different fraudsters who collude the fraud in Meter 4.

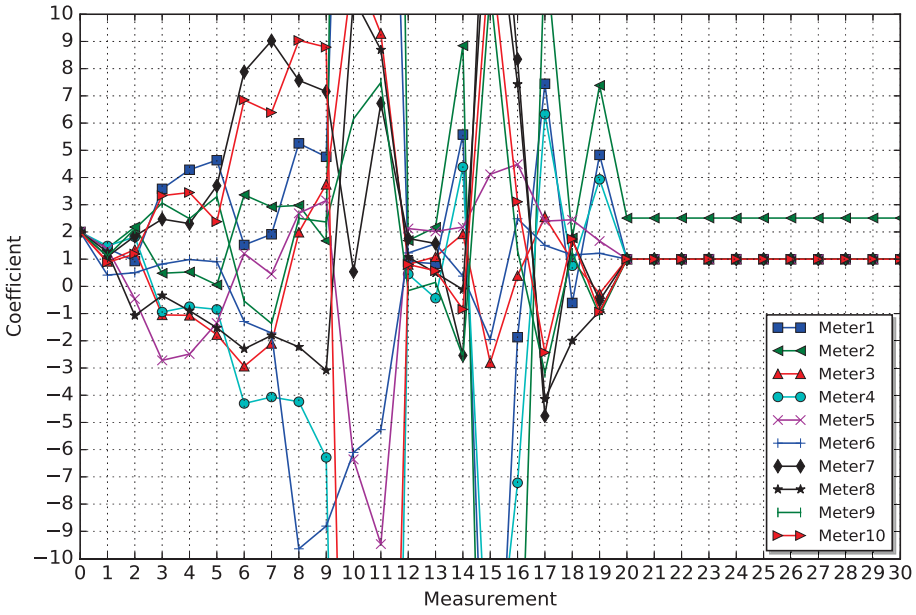

Figure 5.5: The tampered meter detection process in Exp. 2: the converging process of the coefficients of 10 meters. Among these 10 meters, the coefficient of Meter 2 converges to 2.51 while others converge to 1, and this indicates that Meter 2 is a tampered meter.

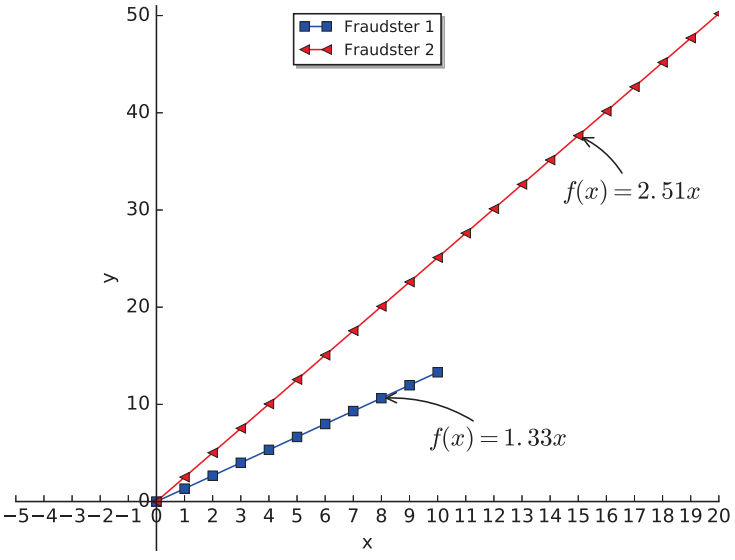

Figure 5.6: The final detection result of CNFD in Exp. 2. CNFD detection shows that two different fraudsters collude the fraud on Meter 2.

Table 5.1: The recorded electricity consumption (kWh) in CNFD - Exp. 1

Meter 1	2	3	4	5	6	7	8	9	10	Observer
2790	3970	5540	2960	3440	9950	5550	4340	5740	6700	51631.2
3400	4200	6510	3620	2360	9970	6030	3590	5310	6840	52626.4
2910	4460	7650	3910	3240	1017	6290	2500	5710	6980	54680.2
3370	3760	6880	3180	4060	1089	6190	6230	7670	8080	61009.6
3690	3940	6600	3580	6090	9780	6830	3280	6200	5320	56097.6
2350	5170	7150	3540	6600	10530	7330	4690	6270	6920	64868.8
3820	3390	7310	4290	3130	9170	6430	4270	6270	6560	59873.8
3120	4930	5550	2180	4110	9790	5820	5200	3350	7570	54279.6
4580	4320	5720	3040	4480	9440	6350	4250	6320	7230	59438.8
2300	4220	4560	3920	3280	9830	5500	4860	6630	5840	55722.4
3350	3900	5850	2990	6120	8760	5650	4720	6670	6220	57877.8
3320	4180	5550	2990	6620	8470	6800	3580	5900	5290	56347.8
2780	3310	5800	3870	4850	8560	6700	3210	3900	4030	51731.4
2980	4900	6560	2520	6130	10350	8000	3620	4660	4900	57694.4
3010	4100	7210	4460	5480	9530	8260	4080	5620	7260	64451.2
4260	3470	7290	5330	4630	9790	8460	3650	4730	6920	65032.6
3610	3640	5740	4140	4870	9730	6630	3590	5870	7420	60290.8
3190	4690	5930	4140	6240	10710	6870	4620	6060	6800	64300.8
3060	5800	6450	3790	3290	11190	7510	4700	5080	6760	62253.8
3660	4050	7010	3610	5160	9810	6670	5520	6250	6440	62584.2

Meter 2 converges to 2.51 while the coefficients of other meters converge to 1, and this indicates that Meter 2 is a tampered meter. We further analyze this meter using CNFD, and we find that this fraud is colluded by two fraudsters. However, the behavior of Fraudster 1 is fully covered by Fraudster 2. Therefore, it is a fully overlapped CNTL fraud. As shown in Fig. 5.6, the behaviors of these two fraudsters are represented by $y = 1.33x$ and $y = 2.51x$, respectively.

5.4.3 Experiment 3: Partially Overlapped CNTL

In this experiment, there are still 10 meters which are monitored by one observer meter. Table 5.3 shows 20 measurements of data of the recorded values of electricity.

The tampered meter detection result is shown in Fig. 5.7. Coefficients of all other meters converge to 1 while the coefficient of Meter 3 converges to 3.11, and this indicates that Meter 3 is a tampered meter. We analyze Meter 3 using CNFD, and find that there are two fraudsters who manipulated this meter. Their manipulation behaviors overlapped

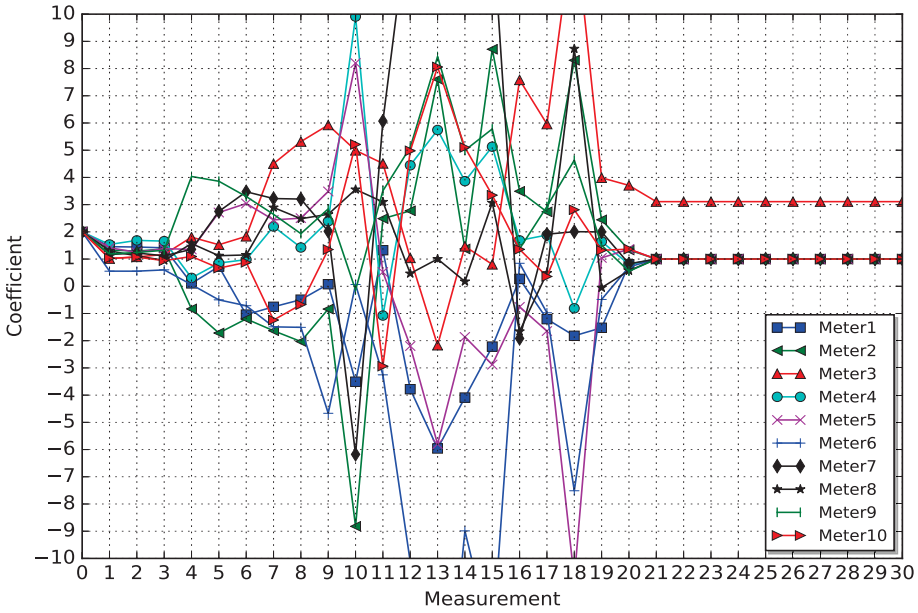

Figure 5.7: The tampered meter detection process in Exp. 3: the converging process of the coefficients of 10 meters. Among these 10 meters, the coefficient of Meter 3 converges to 3.11 while others converge to 1, which indicates that Meter 3 is a tampered meter.

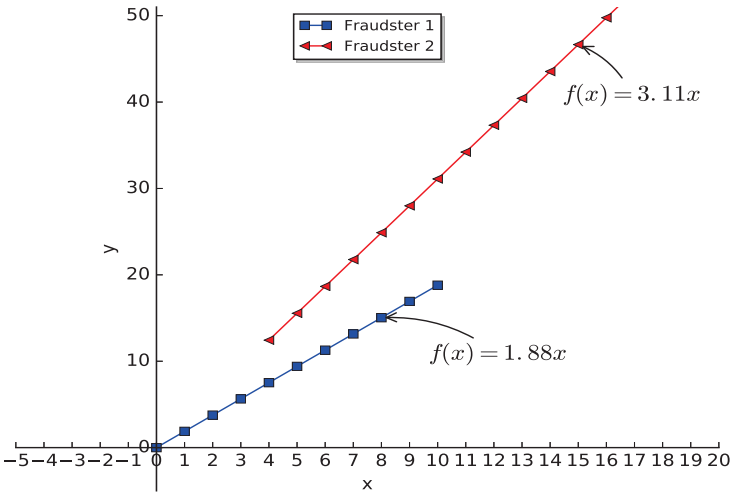

Figure 5.8: The final detection result of CNFD in Exp. 3. CNFD detection shows that there are two different fraudsters who collude the fraud in Meter 3.

Table 5.2: The recorded electricity consumption (kWh) in CNFD - Exp. 2

Meter 1	2	3	4	5	6	7	8	9	10	Observer
3500	3480	6300	2990	3640	9200	5240	4270	5150	6500	51418.4
3420	3960	6730	3250	2950	9580	5770	3380	5790	6880	57689.6
2830	4380	7210	3800	3060	9480	5740	2850	5740	6490	53025.4
3040	4060	7640	3020	3800	1109	6930	6610	7760	8020	63309.8
4170	3510	6370	3740	6000	9970	7380	3380	6240	5350	61410.1
2640	4800	7530	4030	6620	10120	7760	4090	5890	6240	66968
3210	3830	7860	3750	2610	9600	6570	4400	5720	6490	55303.9
2860	4240	5850	2460	4040	9840	6100	4270	3470	7390	56922.4
3760	4200	5580	3610	3880	9930	6040	4350	7080	7100	56916
2750	4230	5030	3720	3550	10540	5270	4970	6730	6020	54205.9
3440	3830	5530	3070	6790	9180	5860	3930	6090	5900	59403.3
3520	3680	6190	3120	6360	7820	6730	3540	6120	4700	57336.8
2120	3150	6300	4160	4480	7940	7320	3190	3690	3930	51036.5
2940	4930	6610	2110	6370	10520	7890	4080	4640	5330	62864.3
3400	3910	6940	4500	5890	9530	7880	3980	4640	6900	63474.1
4410	3320	7130	5050	4860	10120	7950	3300	5530	7500	64183.2
3250	3800	6060	4990	4680	9300	6780	3370	6130	7080	61178
3120	4780	6010	4290	5780	10240	7670	4060	6470	7010	66647.8
2370	5810	7070	3450	3230	11480	7050	4220	5380	6900	65733.1
3580	3580	6710	3670	5010	10270	7170	5030	6420	7130	63975.8

in some time segments, but not in the whole process. Thus, it is a partially overlapped CNTL fraud. These two fraudsters' behaviors are $y = 1.88x$ and $y = 3.11x$ in terms of mathematics, which are shown in Fig. 5.8.

5.4.4 Experiment 4: Combined CNTL

This is the last experiment. In this experiment, we still employ 10 meters and an observer. Table 5.4 shows their recorded data in 20 measurements.

The result of the first step, tampered meter detection, of CNFD is shown in Fig. 5.9. Meter 6 is a tampered meter because the curve of its coefficients finally converges to 1.972. The other 9 meters are normal since the curves of their coefficients finally converge to 1. In the second step, three different fraudsters are identified, and they are represented by $y = 1.45x$, $y = 1.19x$, and $y = 1.98x$, respectively. Fraudster 3 partially overlaps Fraudster 2, while Fraudster 1 and Fraudster 2 are segmented. Thus, it is a combined CNTL fraud shown in Fig. 5.10.

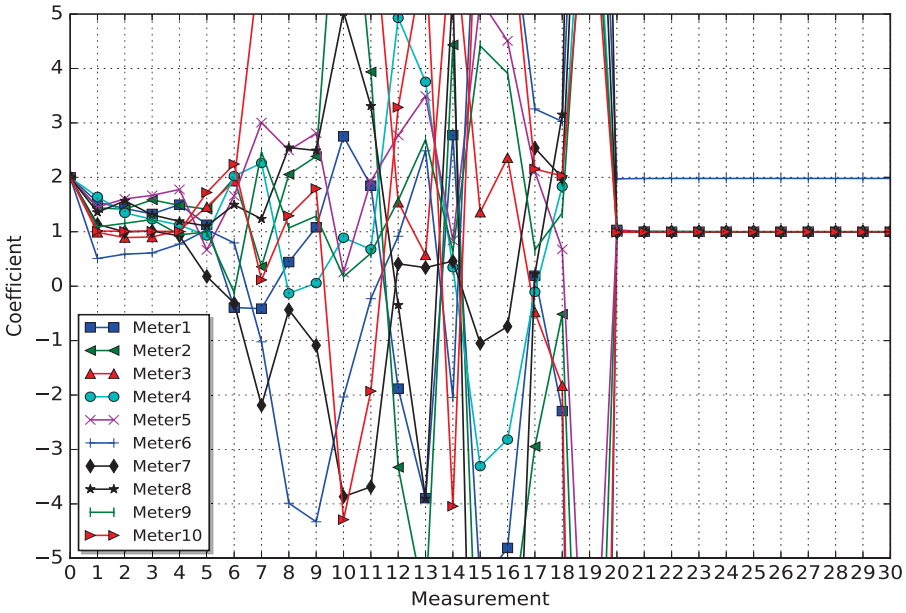

Figure 5.9: The result of the first step, tampered meter detection, of CNFD in Exp. 4. It shows the converging process of the coefficients of 10 meters. The coefficient of Meter 6 converges to 1.972 and the coefficients of other meters converge to 1 showing that Meter 6 is the tampered meter.

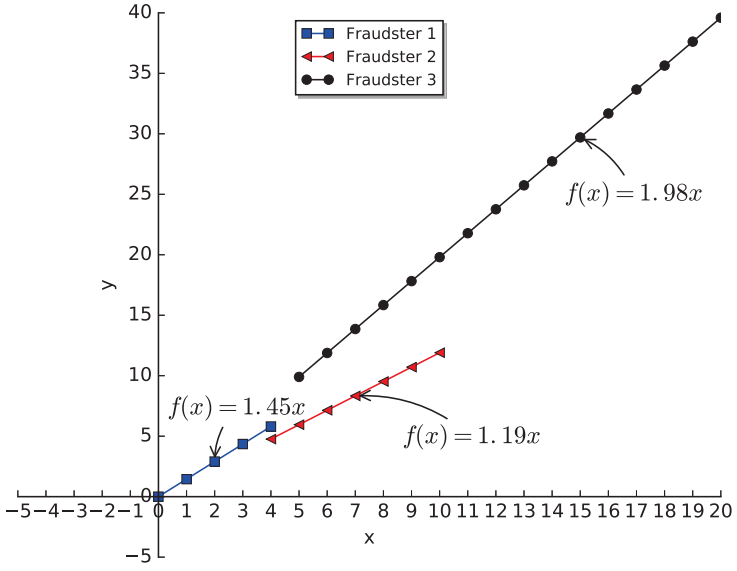

Figure 5.10: The result of CNFD after the second step, fraudster differentiation, in Exp. 4. It shows that there is a CNTL fraud on Meter 6 which are committed by three fraudsters.

Table 5.3: The recorded electricity consumption (kWh) in CNFD - Exp. 3

Meter 1	2	3	4	5	6	7	8	9	10	Observer
3440	4220	6220	2930	3690	9130	5270	4400	5140	6140	56053.6
3550	4180	7050	4190	2690	9670	6000	3300	5840	6810	59484
3530	4650	7600	4140	3400	10140	5710	2760	6330	6440	61388
3330	3470	7560	2720	4030	10360	6600	5900	7560	7630	75111.6
4170	3650	6700	3780	5410	9290	6910	3630	5710	5900	69287
2090	5410	7930	3570	6480	10260	7140	3960	5750	6260	75582.3
3870	3550	7950	4230	3080	9400	6290	4750	5980	6180	72054.5
3440	4390	6370	2220	4430	9210	6340	5160	3230	7520	57915.6
4530	4150	5550	3340	4730	9700	5780	3790	7240	6920	60614
2230	3900	4560	4020	3080	10510	5890	5220	6280	5230	54932.8
2970	3820	6010	3780	5920	9030	6090	4480	6470	5720	66971.1
2980	3770	6360	2730	6220	8460	6570	3740	5910	4400	64559.6
2440	3380	5760	3830	4670	8010	6390	3570	3240	3680	57123.6
3170	4750	6630	2670	5740	10090	8010	3630	5260	4660	68599.3
3080	3370	7190	3930	5540	10260	8220	3790	5440	6480	72470.9
4470	3950	6560	5080	5050	9280	8640	3100	4990	6890	71851.6
3560	4460	5770	4880	4670	9460	6210	2940	5560	7010	66694.7
3590	5040	6500	4430	6200	10390	7680	4310	5920	7000	74775
2900	5440	6970	3080	3940	10850	7200	4750	5520	7200	72556.7
3880	4360	7380	2730	4880	9840	7090	4980	6260	7230	74201.8

5.5 Conclusion

In this chapter, we introduced a potential type of fraud that we recently discovered in Smart Grid. Since this type of fraud is a variant of NTL frauds and mutiple fraudsters co-exist or collaborate to commit a fraud, we named them Colluded NTL (CNTL) frauds. We presented our study on the features of this type of frauds, and categorized them into four types: segmented CNTL frauds, fully overlapped CNTL frauds, partially overlapped CNTL frauds, and combined CNTL frauds. We further proposed a detector, named CNFD, to detect CNTL frauds in Smart Grid. We conducted various experiments and the results showed that CNFD can detect four types of CNTL frauds.

Table 5.4: The recorded electricity consumption (kWh) in CNFD - Exp. 4

Meter 1	2	3	4	5	6	7	8	9	10	Observer
2920	3590	6470	2300	3490	9550	5530	4110	5830	6310	54397.5
3560	3710	6980	3930	2650	9070	6280	2920	5440	6320	54941.5
3100	4540	7140	3160	3230	9600	6380	2210	6020	6540	56240
2660	4350	6860	3230	3540	10410	6800	6200	8210	7430	64374.5
3380	4430	6100	3060	5220	9330	7380	3800	6510	5510	56492.7
2240	5260	7360	4110	6740	10370	7270	4740	5820	6770	70842.6
3670	3500	7920	4300	2570	9590	6260	4040	6330	6850	64428.2
3000	4530	6250	2940	3760	9740	6500	4530	3280	7590	53970.6
4590	4600	5600	3560	4270	9230	5980	4130	6650	7140	57503.7
2920	4210	5150	3430	3190	10260	5460	4680	6910	5710	53869.4
3640	3260	6150	3270	6430	9200	5860	4740	6540	5630	63736
3050	3680	5430	3440	6470	8020	7190	3560	6610	4610	59919.6
2220	3140	5930	4180	4940	8550	6760	2890	3710	3700	54399
2720	4710	5990	2380	6340	10090	7620	3900	5160	4680	63478.2
3480	3870	7280	4670	5270	9500	8380	3980	5220	6920	67880
4228	3948	6678	5348	4780	10188	8088	3668	4818	7480	68976.4
3840	3750	6090	4710	4870	9570	6840	3110	6270	7350	65778.6
3740	5100	6410	4850	5570	9770	7430	4310	5670	6920	69344.6
3060	5520	7180	3630	3900	10590	6920	4240	5580	6480	67478.2
3630	3790	6820	3520	4580	9850	6670	5740	6130	7280	67663

CHAPTER 6

CONCLUSION

In this dissertation, we summarized our recent research on NTL fraud detection in Smart Grid. We first introduced the background of Smart Grid and AMI communication networks. Then, we introduced the research problem - NTL fraud detection including its problem definition and attack model. We studied all the existing solutions that used to address this problem and divided them into five categories. Based on the problems that we found on these solutions, we further propose three novel detectors to solve these problems. The proposed detectors are lightweight and non-traditional. They are built on numerical analysis methods to model adversary behavior which are different from the traditional IDS-based security solutions. They only need a small dataset and do not need detailed energy consumption data which may cause privacy concerns. We presented the experimental results to show the effectiveness of the three detectors. We analyzed the performance of the three detectors theoretically and experimentally. Besides these three detectors, we also published NTL fraud related research in the papers [20, 23, 24]. Some other security related search papers that we published can be found in these articles [22, 27, 30, 33, 37, 42, 63, 64].

In the future, we will study the conjecture of NFD and set up a series of experiments to test its false alarm rate and efficiency in real-world applications. We will further improve the stability of FNFD and validate its performance in the real applications. My future research plan is three fold. First, lightweight and delay-tolerant authentication scheme. Second, fog-computing-driven security analytic. Third, secure time synchronization systems.

REFERENCES

[1] Runge's phenomenon - tallinn university. (n.d.). available at: http://www.tlu.ee/ tonu/Arvmeet/Runge's%20phenomenon.pdf.

[2] Average household electricity use around the world. available at: http://shrinkthatfootprint.com/average-household-electricity-consumption, 2010.

[3] Ansi c12.19-2012. available at: https://www.nema.org/Standards/ComplimentaryDocuments/C12-19-2012-Contents-and-Scope.pdf, 2012.

[4] Smart meter hacking tool released. available at: http://www.zdnet.com/article/smart-meter-hacking-tool-released/, 2012.

[5] Utility-scale smart meter deployments, plans, & proposals. available at:http://www.edisonfoundation.net/iee/Documents/IEE_SmartMeterRollouts_0512.pdf, May 2012.

[6] Emerging markets smart grid: Outlook 2015. available at:http://www.northeast-group.com/reports/Brochure-Emerging%20Markets%20Smart%20Grid-Outlook%202015-Northeast%20Group.pdf, December 2014.

[7] X. Bai. Study of taylor formular approximation precision. *College Mathematics*, 2(4):108–110, August 2016.

[8] R. Berthier and W. H. Sanders. Monitoring advanced metering infrastructures with amilyzer. *Cyber-security of SCADA & industrial control systems*, 2013.

[9] F. Biscarri, I. Monedero, C. Leon, and J. I. Guerrero. A mining framework to detect non-technical losses in power utilities. In *Proceedings of 11th International Conference on Enterprise Information System (ICEIS'09)*, 2009.

[10] I. Hakki Cavdarl. A solution to remote detection of illegal electricity usage via power line communications. *IEEE Transactions on Power Delivery*, 19, October 2004.

[11] M. Comenetz. *Calculus: The Elements*. World Scientific, 2002.

[12] Breno C. Costa, Bruno. L. A. Alberto, André M. Portela, W. Maduro, and Esdras O. Eler. Fraud detection in electric power distribution networks using an ann-based knowledge-discover process. *International Journal of Artificial Intelligence & Applications (IJAIA)*, 4(6):11–23, November 2013.

[13] S.S.S.R. Depuru, L. Wang, and V. Devabhaktuni. Support vector machine based data classification for detection of electricity theft. In *Proceedings of IEEE/PES Power Systems Conference and Exposition (PSCE)*, pages 1–8, March 2011.

[14] Eduardo Werley S. dos Angelos, Osvaldo R. Saavedra, Omar A. Carmona Cortés, and André Nunes de Souza. Detection and identification of abnormalities in customer consumptions in power distribution systems. *IEEE Transactions on Power Delivery*, 26(4):2436–2442, October 2011.

[15] J. Gao, Y. Xiao, J. Liu, W. Liang, , and C. L. P. Chen. A survey of communication/networking in smart grids. *Future Generation Computer Systems*, 28(2):391–404, Febuary 2012.

[16] J. Gao, Y. Xiao, J. Liu, W. Liang, and C. L. P. Chen. A survey of communication/networking in smart grids. *(Elsevier) Future Generation Computer Systems*, 28(2):391–404, 2012.

[17] Jingcheng Gao, Jing Liu, Bharat Rajan, Rahul Nori, Bo Fu, Yang Xiao, Wei Liang, and C. L. Philip Chen. Scada communication and security issues. *Security and Communication Networks Security Comm*, 7(1):175–194, 2014.

[18] D.J. Gaushell and H.T. Darlington. Supervisory control and data acquisition. *Proceedings of the IEEE*, 75(3):1645–1658, 2005.

[19] Georges Habrail and Alice Barard. Individual household electric power consumption data set. available at:https://archive.ics.uci.edu/ml /datasets/Individual+household+electric+power+consumption, 2012.

[20] Wenin Han and Yang Xiao. Big data security analytic for smart grid with fog nodes. In *In Proceedings of the 9th International Conference on Security, Privacy and Anonymity in Computation, Communication and Storage (SpaCCS 2016)*, pages 59–69, November 2016.

[21] Wenin Han and Yang Xiao. CNFD: A novel scheme to detect colluded non-technical loss fraud in smart grid. In *The 11th International Conference on Wireless Algorithms, Systems, and Applications (WASA 2016)*, pages 47–55, August 2016.

[22] Wenin Han and Yang Xiao. CO_2: A fault-tolerant relay node deployment strategy for throwbox-based dtns. In *In Proceedings of the 11th International Conference on Wireless Algorithms, Systems, and Applications (WASA 2016)*, pages 37–46, August 2016.

[23] Wenin Han and Yang Xiao. Combating TNTL: Non-technical loss fraud targeting time-based pricing in smart grid. In *The 2nd International Conference on Cloud Computing and Security (ICCCS 2016)*, July 2016.

[24] Wenin Han and Yang Xiao. Non-technical loss fraud in advanced metering infrastructure in smart grid. In *The 2nd International Conference on Cloud Computing and Security (ICCCS 2016)*, 2016.

[25] Wenin Han and Yang Xiao. Privacy preserving for v2g networks in smart grid: A survey. *Computer Communications*, 91-92:17–28, 2016.

[26] Wenlin Han and Yang Xiao. NFD: A practical scheme to detect non-technical loss fraud in smart grid. In *Proceedings of the 50th International Conference on Communications (ICC'14)*, pages 605–609, June 2014.

[27] Wenlin Han and Yang Xiao. IP^{2}DM for V2G networks in smart grid. In *Proceedings of the 50th International Conference on Communications (ICC'15)*, pages 782–787, June 2015.

[28] Wenlin Han and Yang Xiao. Design a fast non-technical loss fraud detector in smart grid. *(Wiley Journal of) Security and Communication Networks*, October 2016.

[29] Wenlin Han and Yang Xiao. FNFD: A fast scheme to detect and verify non-technical loss fraud in smart grid. In *International Workshop on Traffic Measurements for*

Cybersecurity (WTMC'16), DOI: http://dx.doi.org/10.1145/2903185.2903188, pages 24–34, May 30 - June 3 2016.

[30] Wenlin Han and Yang Xiao. IP^{2}DM: Integrated privacy-preserving data management architecture for smart grid v2g networks. *Wireless Communications and Mobile Computing*, September 2016.

[31] Wenlin Han and Yang Xiao. NFD: Non-technical loss fraud detection in smart grid. *Computers & Security*, November 2016.

[32] Wenlin Han and Yang Xiao. A novel detector to detect colluded non-technical loss fraud in smart grid. *Computer Networks*, October 2016.

[33] Wenlin Han, Wei Xiong, Yang Xiao, M. Ellabidy, A. V. Vasilakos, and Naixue Xiong. A class of non-statistical traffic anomaly detection in complex network systems. In *Proceedings of the 32nd International Conference on Distributed Computing Systems Workshops (ICDCSW'12)*, pages 640–646, June 2012.

[34] Monson H. Hayes. Recursive least squares. In *Statistical Digital Signal Processing and Modeling*, chapter 9.4, page 154. Wiley, 1996.

[35] Shih-Che Huang, Yuan-Liang Lo, and Chan-Nan Lu. Non-technical loss detection using state estimation and analysis of variance. *IEEE Transactions on Power Systems*, 28(3):2959–2966, August 2013.

[36] Paria Jokar, Nasim Arianpoo, and Victor C. M. Leung. A survey on security issues in smart grids. *Security and Communication Networks*, 9:262–273, June 2012.

[37] Julius Jow, Yang Xiao, and Wenlin Han. A survey of intrusion detection in smart grid. *International Journal of Sensor Networks*, 2017.

[38] G. Kalogridis, S.Z. Denic, T. Lewis, and R. Cepeda. Privacy protection system and metrics for hiding electrical events. *International Journal of Security and Networks*, 6(1):14–27, 2011.

[39] F. Li, B. Luo, and P. Liu. Secure and privacy-preserving information aggregation for smart grids. *International Journal of Security and Networks*, 6(1):28–39, 2011.

[40] Chia-Hung Lin, Shi-Jaw Chen, Chao-Lin Kuo, and Jian-Liung Chen. Non-cooperative game model applied to an advanced metering infrastructure for non-technical loss screening in micro-distribution systems. *IEEE Transactions on Smart Grid*, 5(5):2468–2469, September 2014.

[41] J. Liu, Y. Xiao, S. Li, W. Liang, and C. L. P. Chen. Cyber security and privacy issues in smart grids. *IEEE Communications Surveys & Tutorials*, 14(4):981–997, Fourth Quarter 2012.

[42] Jing Liu, Wenlin Han, and Yang Xiao. Enhancements of temporal accountability in medical sensor networks. *Ad hoc & sensor wireless networks*, 2017.

[43] S. Ma, Y. Yang, Y. Qian, H. Sharif, and M. Alahmad. Energy harvesting for wireless sensor networks: applications and challenges in smart grid. *International Journal of Sensor Networks*, 21(4):226–241, 2016.

[44] Patrick McDaniel and Sean W. Smith. Security and privacy challenges in the smart grid. *IEEE Security & Privacy*, 7(3):75–77, 2009.

[45] Stephen McLaughlin, Brett Holbert, Saman Zonouz, and Robin Berthier. AMIDS: A multi-sensor energy theft detection framework for advanced metering infrastructures. In *Proceedings of the 2012 IEEE Third International Conference on Smart Grid Communications (SmartGridComm'12)*, pages 354–359, November 2012.

[46] N. Mohammad, A. Baru, and M.A. Arafat. A smart prepaid energy metering system to control electricity theft. In *Proceedings of the Int'l Conf. on Power, Energy and Control*, pages 562–565, 2013.

[47] J. Mu, W. Song, W. Wang, and B. Zhang. Self-healing hierarchical architecture for zigbee network in smart grid application. *International Journal of Sensor Networks*, 17(2):130–137, 2015.

[48] U.S. Department of Energy. The smart grid: an introduction. available at: http://energy.gov/oe/downloads/smart-grid-introduction-0. Accessed: 02/09/2016.

[49] A. Pasdar and S. Mirzakuchaki. A solution to remote detecting of illegal electricity usage based on smart metering. In *Proceedings of the 2nd Int'l workshop on Soft Computing Applications*, pages 163–167, 2007.

[50] Perumalraja Rengaraju, Shunmugham R. Pandian, and Chung-Horng Lung. Communication networks and non-technical energy loss control system for smart grid networks. In *Proceedings of the 2014 IEEE Innovative Smart Grid Technologies - Asia (ISGT ASIA)*, pages 418–423, May 2014.

[51] Patil S, Gopal Pawaskar, and Kirtikumar Patil. Electrical power theft detection and wireless meter reading. *Int'l Journal of Innovative Research in Science, Eng. and Technology*, 2:114–119, 2013.

[52] K. Silverstein. India and u.s. share energy woes: Stealing electricity. available at:http://www.forbes.com/sites/kensilverstein/2012/08/05/india-and-u-s-share-energy-woes-stealing-electricity/,
2012.

[53] SATEC Power Solutions. Accuracy class: a small s that makes a big difference. available at: http://www.satec-global.com/sites/default/files/ApplicationNote-Accuracy-Class-Dec2012.pdf,
2012.

[54] M. Spivak. *Calculus (3rd ed.)*. Houston, TX: Publish or Perish, 1994.

[55] R. Targosz. Electricity theft - a complex problem. available at: http://www.leonardo-energy.org/electricity-theft-complex-problem, July 2009.

[56] K. Tweed. Fbi finds smart meter hacking surprisingly easy. available at:http://www.greentechmedia.com/articles/read/fbi-finds-smart-meter-hacking-surprisingly-easy/,
2012.

[57] J.V. Wijayakulasooriya, D.M.I.S. Dasanayake, P.I. Muthukumarana, H.M.P.P. Kumara, and L.A.D.S.D. Thelisinghe. Remotely accessible single phase energy measuring system. In *Proceedings of the 1st Int'l Conf. on Industrial and Information Systems*, pages 304–309, 2006.

[58] Xiaofang Xia, Wei Liang, Yang Xiao, and Meng Zheng. BCGI: A fast approach to detect malicious meters in neighborhood area smart grid. In *Proceedings of the 50th International Conference on Communications (ICC'15)*, pages 7228–7233, June 2015.

[59] Xiaofang Xia, Wei Liang, Yang Xiao, Meng Zheng, and Zhifeng Xiao. Difference-comparison-based approach for malicious meter inspection in neighborhood area smart grids. In *Proceedings of the 50th International Conference on Communications (ICC'15)*, pages 802–807, June 2015.

[60] Z. Xiao, Y. Xiao, and D. Du. Building accountable smart grids in neighborhood area networks. In *Proceedings of the IEEE Global Telecommunications Conference 2011 (GLOBECOM'11)*, pages 1–5, December 2011.

[61] Z. Xiao, Y. Xiao, and D. Du. Exploring malicious meter inspection in neighborhood area smart grids. *IEEE Transactions on Smart Grid*, 4(1):214–226, March 2013.

[62] Z. Xiao, Y. Xiao, and D. Du. Non-repudiation in neighborhood area networks for smart grid. *IEEE Communications Magazine*, 51(1):18–26, January 2013.

[63] Junhan Yang, Bo Su, Chaoping Guo, Wenlin Han, and Yang Xiao. Provably secure cl-kem based password-authenticated key exchange protocol. *International Journal of Sensor Networks*, 2017.

[64] Lei Zeng, Yang Xiao, Hui Chen, Bo Sun, and Wenlin Han. Computer operating system logging and security issues: A survey. *(Wiley Journal of) Security and Communication Networks*, October 2016.

APPENDIX A

PROOF OF THEOREM 3.1

Proof. Suppose that for a given Meter i, its approximation polynomial is $Q_i(x)$ with the order of m, its approximation polynomial is $P_i(x)$ with the order of $m+1$, and its original function is $f_i(x)$. According to Eq. (3.13), the error of $Q_i(x)$ is as follows:

$$R_{i,m}(x) = \frac{f^{(m+1)}(\xi)}{(m+1)!}(x-x_0)^{m+1}, \xi \in [x_0, x]. \tag{A.1}$$

Lemma A.1. *When* $\lim_{m\to\infty} R_{i,m}(x) = 0$*, the accuracy of* $P_i(x)$ *is always higher than* $Q_i(x)$*.*

Proof. For

$$f_i(x) = Q_i(x) + R_{i,m}(x), \tag{A.2}$$

and $Q_i(x) = \sum_{j=0}^{m} \frac{f_i^{(j)}(x_0)}{j!}(x-x_0)^j$, $R_{i,m}(x)$ can be given as

$$R_{i,m}(x) = \frac{f_i^{(m+1)}[x_0 + \theta(x-x_0)]}{(m+1)!}(x-x_0)^{m+1}, 0 < \theta < 1. \tag{A.3}$$

Putting it into Eq. (A.2), we get

$$\begin{aligned} f_i(x) = & \sum_{j=0}^{m} \frac{f_i^{(j)}(x_0)}{j!}(x-x_0)^j + \frac{f_i^{(m+1)}[x_0 + \theta(x-x_0)]}{(m+1)!}. \\ & (x-x_0)^{m+1} \end{aligned} \tag{A.4}$$

For $f_i^{(m+1)}(x)$, apply mean-value theory [11] in the close interval $[x_0, x_0 + \theta(x-x_0)]$, we get

$$\frac{f_i^{(m+1)}[x_0 + \theta(x-x_0)] - f_i^{(m+1)}(x_0)}{\theta(x-x_0)} = f_i^{(m+2)}(\xi). \tag{A.5}$$

Thus,

$$f_i^{(m+1)}[x_0+\theta(x-x_0)] = \theta(x-x_0)f_i^{(m+2)}(\xi) + f_i^{(m+1)}(x_0). \tag{A.6}$$

Put Eq. (A.6) into Eq. (A.4) to obtain:

$$f_i(x) = Q_{i,(m+1)}(x) + \frac{\theta f_i^{(m+2)}(\xi)}{(m+1)!}(x-x_0)^{m+2}. \tag{A.7}$$

From Eq. (A.2), we get

$$\begin{aligned} f_i(x) = Q_{i,(m+1)}(x) + \frac{f_i^{(m+2)}[x_0+\theta_1(x-x_0)]}{(m+2)!}(x-x_0)^{m+2}, \\ 0<\theta_1<1. \end{aligned} \tag{A.8}$$

Comparing Eqs. (A.7) and (A.8), the following can be obtained

$$\frac{\theta f_i^{(m+2)}(\xi)}{(m+1)!}(x-x_0)^{m+2} = \frac{f_i^{(m+2)}[x_0+\theta_1(x-x_0)]}{(m+2)!}.$$

$$(x-x_0)^{m+2}.$$

According to [7], suppose $x \to x_0$.

$$\begin{aligned} &\because f_i^{(m+2)}(x_0) \neq 0, \textit{ and } f_i^{(m+2)}(x) \textit{ is continuous}, \\ &\therefore \lim_{x\to x_0}\theta = \frac{1}{m+2}. \end{aligned}$$

When x_0 is in a sufficiently small neighborhood, $\theta \approx \frac{1}{m+2}$, and

$$f_i(x) \approx Q_{i,m}(x) + \frac{f_i^{(m+1)}(x_0+\frac{x-x_0}{m+2})}{(m+1)!}(x-x_0)^{m+1}. \tag{A.9}$$

The right side of Eq. (A.9) is actually the approximation of $f_i(x)$ with $m+1$ order. That is

$$P_i(x) = Q_{i,m}(x) + \frac{f_i^{(m+1)}(x_0+\frac{x-x_0}{m+2})}{(m+1)!}(x-x_0)^{m+1}, \tag{A.10}$$

and $Q_{i,m}(x) = Q_i(x)$. Thus,

$$
\begin{aligned}
& f_i(x) - P_i(x) = f_i(x) - Q_i(x) - \frac{f_i^{(m+1)}(x_0 + \frac{x-x_0}{m+2})}{(m+1)!}. \\
& (x-x_0)^{m+1} \\
=& \frac{f_i^{(m+1)}(x_0)}{(m+1)!}(x-x_0)^{m+1} + \frac{f_i^{(m+2)}[x_0 + (\theta_1(x-x_0))]}{(m+2)!}. \\
& (x-x_0)^{m+2} - \frac{f_i^{(m+1)}(x_0 + \frac{x-x_0}{m+2})}{(m+1)!}(x-x_0)^{m+1} \\
=& \frac{f_i^{(m+2)}[x_0 + (\theta_1(x-x_0))]}{(m+2)!}(x-x_0)^{m+2} - \frac{(x-x_0)^{m+1}}{(m+1)!}. \\
& \int_{x_0}^{x_0 + \frac{x-x_0}{m+2}} f^{m+2}(t)dt \\
=& \frac{(x-x_0)^{m+1}}{(m+1)!} \left\{ \frac{f_i^{m+2}[x_0 + \theta_1(x-x_0)]}{m+2}(x-x_0) \right. \\
& \left. - \int_{x_0}^{x_0 + \frac{x-x_0}{m+2}} f^{m+2}(t)dt \right\}, \theta_1 \in (0,1).
\end{aligned}
\tag{A.11}
$$

According to the mean value theorem of integrals, there exists $\eta \in (x_0, x_0 + \frac{x-x_0}{m+2})$, and

$$
\begin{aligned}
f_i(x) - P_i(x) = & \frac{(x-x_0)^{m+2}}{(m+2)!}\{f^{(m+2)}[x_0 + \theta_1(x-x_0)] \\
& - f^{(m+2)}(\eta)\}.
\end{aligned}
\tag{A.12}
$$

- When $f^{(m+2)}[x_0 + \theta_1(x-x_0)] - f^{(m+2)}(\eta) \neq 0$, $f_i(x) - P_i(x) = \mathcal{O}((x-x_0)^{m+2})$;
- When $f^{(m+2)}[x_0 + \theta_1(x-x_0)] - f^{(m+2)}(\eta) = 0$, $f_i(x) - P_i(x) = o((x-x_0)^{m+2})$.

Therefore, the accuracy of $P_i(x)$ is always higher than $Q_i(x)$. □

Lemma A.2. *When* $\lim_{m\to\infty} R_{i,m}(x) = +\infty$, *the accuracy of* $P_i(x)$ *is not always higher than* $Q_i(x)$.

Proof. We prove it with a counterexample.

Consider the following function

$$f_i(x) = \frac{2}{2 + 33x^2}. \tag{A.13}$$

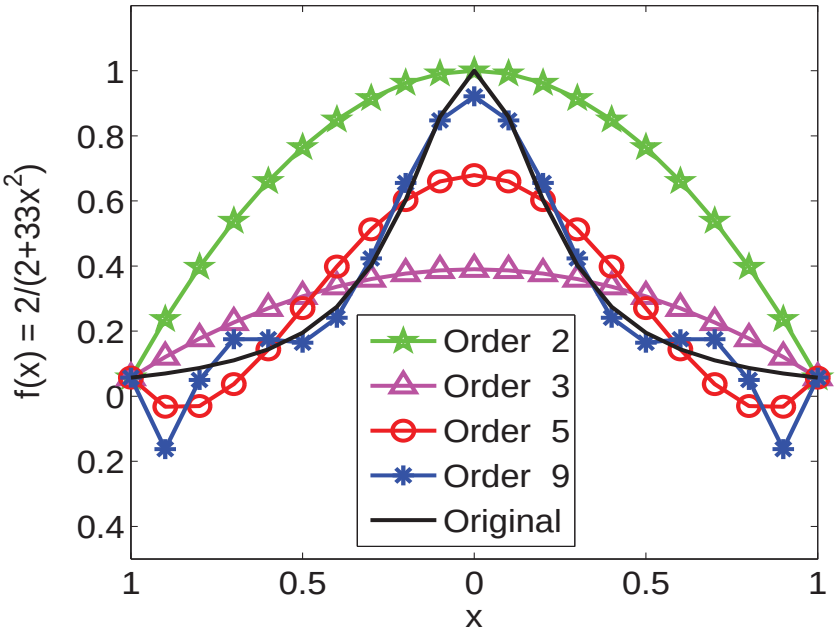

Figure A.1: The curves of approximation polynomials with different orders of the same function $f_i(x) = \frac{2}{2+33x^2}$. A counter example to illustrate a higher order does not always improve accuracy.

Fig. A.1 shows its approximation polynomials with order 2, order 3, order 5, and order 9, respectively. The order 5 polynomial, the red curve, is a better approximation than the order 2, the green curve, and the order 3, the magenta curve. Most of the order 9 curve, the blue one, is closer to the original function than the order 5, the red curve. However, it oscillates at the end of the interval, i.e. close to -1 and 1. The reason is that the upper bound for the approximation error grows to infinity with m [1].

$$f_i(x) - Q_i(x) = \frac{f^{(m+1)}(\xi)}{(m+1)!} \prod_{j=1}^{m+1} (x - x_j), \xi \in [x_0, x], \tag{A.14}$$

and for some $\xi \in (-1, 1)$,

$$\begin{aligned} \max_{-1\le x\le 1} |f_i(x) - P_i(x)| \le & \max_{-1\le x\le 1} \frac{f_i^{(m+1)}(x)}{(m+1)!} \cdot \\ & \max_{-1\le x\le 1} \prod_{j=1}^{m+1} (x - x_j). \end{aligned} \tag{A.15}$$

Thus,

$$\lim_{m\to\infty} \big(\max_{-1\le x\le 1} |f_i(x) - P_i(x)| \big) = +\infty. \tag{A.16}$$

Because of the oscillation, a meter's polynomial of a higher order could be less accurate than its polynomial of a lower order, especially when the range of the measured electricity - x, is close to the oscillation range. Therefore, when $\lim_{m\to\infty} R_{i,m}(x) = +\infty$, the accuracy of $P_i(x)$ is not always higher than $Q_i(x)$. □

Based on Lemmas A.1 and A.2,

1. When $\lim_{m\to\infty} R_{i,m}(x) = 0$, the accuracy of $P_i(x)$ is always higher than $Q_i(x)$;
2. When $\lim_{m\to\infty} R_{i,m}(x) = +\infty$, the accuracy of $P_i(x)$ is not always higher than $Q_i(x)$.

A polynomial with a higher order m does not always improve the accuracy of its approximation. Theorem 3.1 has then been established. □